Materials and Methods

Animals

Genomic DNA was isolated from RBCs for mapping analysis from the nurse shark family as previously described (21). The procedure of animal use was reviewed and approved by the Institutional Animal Care and Use Committee at the University of Maryland.

Bacterial artificial chromosome library screening

The 17 bacterial artificial chromosome (BAC) filters with 11-fold genomic coverage (22) were screened with radiolabeled full-length *β2M* or *ring3* probes under high-stringency conditions (23). Membranes were exposed to x-ray film for various lengths of time to obtain positive signals and the desired background. Putative positive clones were then re-spotted on nylon membranes for colony hybridization and tested by Southern blotting to confirm true positives. BAC insert DNA was isolated using the PhasePrep BAC DNA kit (Sigma-Aldrich), and the sequence was determined by shotgun sequencing at the sequencing facility at Tokai University with 7.5× coverage.

Sequence alignment and phylogenetic tree

Amino acid sequences of constant-1 (C1)-IgSF domains were aligned using the ClustalX2 program with minor adjustments. A rooted neighbor-joining (NJ) bootstrapped (1000 runs) phylogenetic tree (24) was constructed, and the consensus tree was then viewed with the TreeView program (25).

Database searches

Genome synteny in various species was retrieved and analyzed from publicly available Web sites as noted. Genes from mouse, chicken, human, opossum, and zebrafish were retrieved from GenBank (http://www.ncbi.nlm.nih.gov), and information on other genomes was retrieved from the following Web sites: elephant shark genome (http://blast.fugu-sg.org/); *Anolis* genome (http://genome.ucsc.edu/cgi-bin/hgGateway?db=anoCar1); *Xenopus* genome (http://genome.jgi-psf.org/Xentr4/Xentr4.home.html); and *Fugu* genome (http://genome.jgi-psf.org/Takru4/Takru4.home.html).

In-house EST collection

We constructed the cDNA library using the Gateway System (Invitrogen) from adult nurse shark pancreas. To eliminate Ig genes, we first hybridized with Ig H and L chain probes under high-stringency conditions. Negative colonies (~8000) were then manually picked and sequenced from the vector end. All draft sequences were blastx searched against GenBank databases, and we obtained ~1150 sequences not specific to the pancreatic enzymes (Y. Ohta and M.F. Flajnik, personal observations).

Single-strand conformation polymorphism analysis

Nurse shark *ring3* primers were designed based on the sequence obtained from BAC GC_614H19 clone. Multiple primers were tried, and we selected the primer set anchoring exons 4 and 5 for the single-strand conformation polymorphism (ssCP) analysis. The primers were exon 4 forward, 5′-GTTAACACCTGCACCAAAAT-3′; and exon 5 reverse, 5′-ATTGGGACCTGAGACACAGT-3′. PCR was performed at 94°C for 4 min, followed by 35 cycles of 94°C for 1 min, 62°C for 1 min, and 72°C for 1 min, with a final extension of 72°C for 10 min using 2–500 ng genomic DNA as template. The ~1340-bp PCR product was cleaned by gel extraction. The ssCP gel (0.5× MDE gel; Cambrex Bio Science Rockland) was run at 16°C for 30 h in 0.6× Tris/borate/EDTA buffer with 1 W constant power.

Allele-specific PCR

Nurse shark *β2M* sequences were obtained from family 2 with known MHC haplotypes. PCR was performed using a forward primer in intron 2 (NSB2mint2For: 5′-TTACACATCACCACCACCTC-3′) and a reverse primer designed from the IgSF exon (exon 3) (NSB2mex3Rev: 5′-GATTGATTCAGTAGC-3′). We amplified *β2M* gene fragments from several animals carrying different maternal and paternal haplotype combinations to find allele-specific polymorphisms. After we identified a two-nucleotide deletion in intron 2 in the paternal haplotype in animals belonging to groups "i" and "j" (*p3*), allele-specific primers were designed for each gene in which deletions are positioned at the third and fourth nucleotide positions at the 3′-end of primers. PCR was performed using a combination of allele-specific and NSB2mex3Rev primers at 94°C for 4 min, followed by 35 cycles of 94°C for 1 min, 58°C for 1 min, and 72°C for 1 min, with a final extension of 72°C for 10 min using 2–500 ng genomic DNA as template. We also found animals with the "CC-deletion" allele in two other families (1 and 3).

Northern blotting

Total RNA was isolated from various nurse shark tissues by using the TRIzol reagent (Invitrogen). Twenty micrograms of total RNA was electrophoresed and blotted onto Optitran Nitrocellulose membrane (Schleicher & Schuell). The membrane was hybridized with full-length shark probes and washed under high-stringency conditions (23).

Southern blotting

Genomic DNA (10 μg) was digested with various restriction enzymes to obtain useful RFLP in unrelated sharks with multiple enzymes. The IgSF exon was used to determine the number of loci for *β2m* under high-stringency conditions (23). Hybridization with MHC class I leader and α1 domain probe was performed under low-stringency conditions (23). To determine the MHC groups in the shark family 2, we digested genomic DNA with HindIII and hybridized with radiolabeled probe including the leader–α1 domains of MHC class I under high-stringency conditions.

Sequence analysis of MHC class I alleles and sire designation

MHC class I sequences were obtained from PCR amplification with primers from α1 domain forward, 5′-GGTCGGTTATGTGGATGATC-3′; and α2 domain reverse, 5′-TTGCAGCCACTCGATACA-3′. PCR amplification was performed for 4 min at 94°C, followed by 35 cycles of 94°C for 1 min, 56°C for 1~2 min, 72°C for 1 min, and a final extension at 72°C for 10 min. An ~550-bp fragment amplicon was cloned into the pCRII TA cloning vector (Invitrogen), and individual clones were sequenced. Nurse shark families 2 and 3 were genotyped using 12 DNA microsatellite markers and assigned sires (E.J. Heist, J.C. Carrier, H.L. Pratt, and T.C. Pratt, submitted for publication).

Statistical analysis of linkage

We used parametric linkage analysis to formally assess the evidence for linkage of *β2M* to the MHC region in the offspring of deletion-carrying sires. This approach assesses the odds of the likelihood of obtaining the observed data set if the two loci are linked versus if the loci are not linked, showing as a log of the odds (LOD) score. The paternal sibships were determined based on consolidated data from combination of Southern blotting, sequencing of MHC class Ia alleles, and microsatellite analyses (shown in Table I).

The LOD score is calculated as follows when parental phase (linkage status) is known: $\mathrm{LOD} = \log 10\ \{[(\theta)^{R}(1-\theta)^{NR}]/(0.5)^{R+NR}\}$, where θ is the recombination fraction, *NR* is the number of nonrecombinant offspring, and *R* is the number of recombinant offspring.

Because the parental phase was unknown in the current study due to a lack of grandparental genotypes, a phase ambiguous LOD score was first calculated for each family by taking the log of the average odds for the two possible phases (1 and 2 in Table I), and the resulting LOD scores were then summed over the two families to obtain the LOD score at a given recombination fraction. LOD scores were calculated at recombination fractions between 0 and 0.5 to obtain the recombination fraction where the LOD score was maximized (26). The corresponding *p* value was calculated using a one-sided χ^2 test of LOD ×2 ($\log_e 10$) (27).

Results

Characterization of nurse shark β2M

Cartilaginous fish are the oldest living vertebrates having an adaptive immune system centered upon Ig, TCR, and MHC (1). When it was suggested that class I and class II genes may have evolved in separate linkage groups from studies of teleost fish (28), we demonstrated in family studies that the two MHC classes were closely linked in two shark species, nurse shark and banded houndshark (21). To gain further insight into the primordial MHC organization, we have isolated many shark genes associated with adaptive immunity, including *β2M*. The full-length *β2M* clone was found in an in-house EST collection (GenBank accession number HM625831), as well as from a previously published genomic sequence (GenBank accession number GQ865623) (29), and the deduced amino acid sequence was aligned with β2M from other species (S1). As was noted in previous studies, evolutionarily

conserved residues are either found in all C1-IgSF (or just IgSF) domains (29, 30) or are predicted to be at class Iα-chain interaction sites (31). Some cartilaginous fish β2M have potential N-glycosylation sites that are rare in tetrapods but present in several bony fish species (32). Consistent with previous studies (33, 34), phylogenetic tree analysis revealed that cartilaginous fish β2M clustered with the orthologous proteins and to the IgSF domains of MHC class IIA/DMA, suggesting that they share the most recent common ancestor (Fig. 1*A*). Also consistent with previous studies (33), the IgSF domains of class IIB and class Ia shared the most recent common ancestor. *β2M* expression pattern seems to coincide with MHC class I expression (Fig. 1*B*).

Mapping of β2M *to the MHC in family studies*

Two families of nurse sharks previously were used to map several genes to the MHC (21, 36, 37). All of these families showed multiple paternity, at least five fathers in family 1 and seven in family 2. Southern blotting analysis using many restriction enzymes demonstrated that *β2M* is a single-copy gene (five representative digestions are shown in Fig. 1*C*); unfortunately, no RFLPs were obtained to test the linkage status, and thus we sequenced the gene from animals with different MHC haplotypes, hoping to find polymorphisms. A two-nucleotide deletion was detected in one of the paternal *β2M* alleles "*p3*" from groups "i" (p3/m2) and "j," (p3/m1) from family 2 with 39 members (Fig.

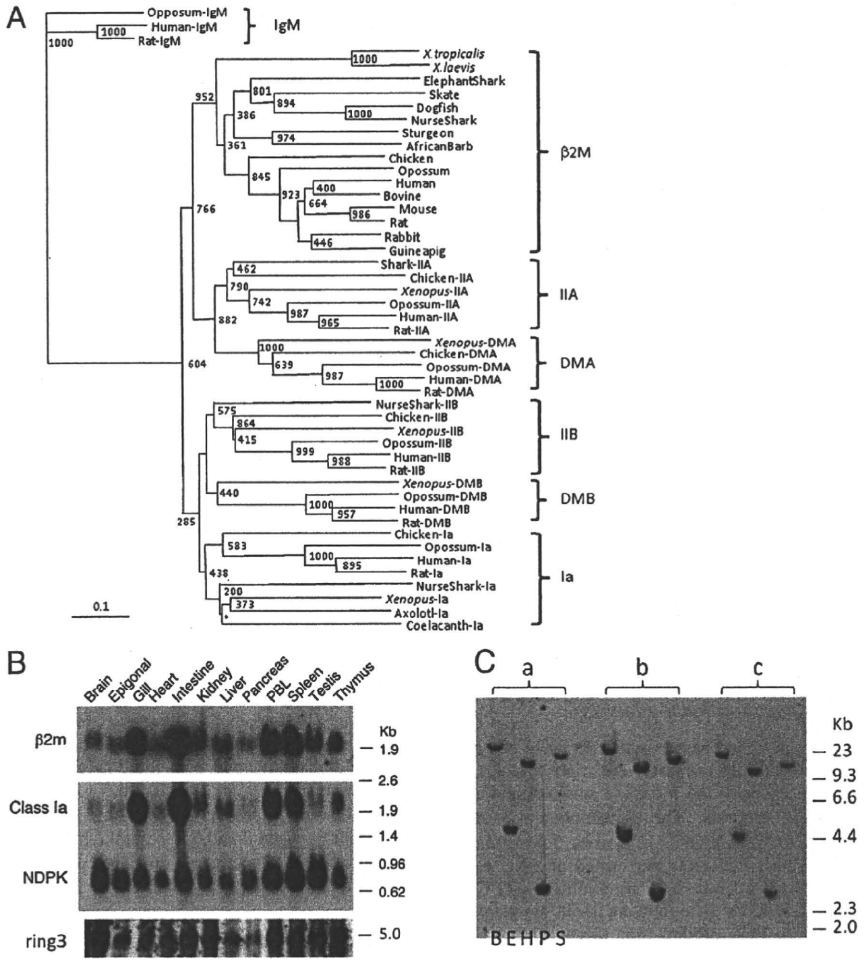

FIGURE 1. *A*, Phylogenetic tree analysis of β2M. GenBank accession numbers used for this analysis are as follows. β2M: M17987 (human), X69084 (bovine), NM_009735 (mouse), Y00441 (rat), P01885 (rabbit), P01886 (guinea pig), M84767 (chicken), P21612 (turkey), AAM98336 (opossum), BQ389924 (*X. tropicalis*), AAF37230 (*X. laevis*), L05536 (carp), NP_571238 (zebrafish), L63534 (trout), CAA10761 (cod), AAG17535 (salmon), CAB61324 (Siberian sturgeon), AAN40738 (Japanese flounder), CAD44965 (African barb), O42197 (catfish), CA330181 (*Fugu*), AAN62852 (skate), and CX197532 (dogfish). Class IIa: AAF66123 (nurse shark), AAL58430 (*X. laevis*), AAA59760 (human), AAV40625 (rat), NP_001001762 (chicken), XP_001376764 (opossum). Class IIb: AAF82681 (nurse shark), AAB86437 (human), NP_001008884 (rat), BAA02845 (*X. laevis*), NP_001038144 (chicken), AAB68822 (opossum). Class Ia: BAD92354 (human), AAC53397 (rat), AAL59857 (nurse shark), NP_001079241 (*X. laevis*), AAG28835 (chicken), NP_001165308 (opossum). IgM: AAD21191 (opossum), P01871 (human), AAH92586 (rat). DMB: ABB85336 (*X. laevis*), NP_002109 (human), NP_942035 (rat). DMA: NP_006111 (human), NP_942036 (rat), ACY01474 (chicken), XP_001377359 (opossum). The NJ tree was rooted with the fourth constant IgSF domains of IgM, and bootstrapping analysis was done after 1000 runs. Values are noted at the branch nodes, and the asterisk (*) indicates no significant value. The scale indicates divergence time (genetic distance). Teleost fish that underwent a third round of genome expansion ("3R") are omitted from this analysis because the sequences were more divergent and skewing the tree topology. DM genes have not been identified in any fish. *B*, Expression profiles of *β2M*, class Ia, and *ring3* via Northern blotting. Twenty micrograms of total RNA isolated from various nurse shark tissues was loaded onto the gel, blotted, and hybridized with full-length shark *β2M* and *ring3* probes and washed under high-stringency conditions (23). Nucleoside-diphosphate kinase (*NDPK*) (35) was used as a loading control. *C*, There is only one *β2M* locus in the nurse shark genome. Genomic Southern blot analysis was performed under low-stringency conditions (23) using the IgSF exon with three wild sharks (*a*, *b*, *c*) whose DNA was digested with five different restriction enzymes (from *left* to *right*: *Bam* HI, *Eco* RI, *Hin* dIII, *PST* I, and *Sac* I).

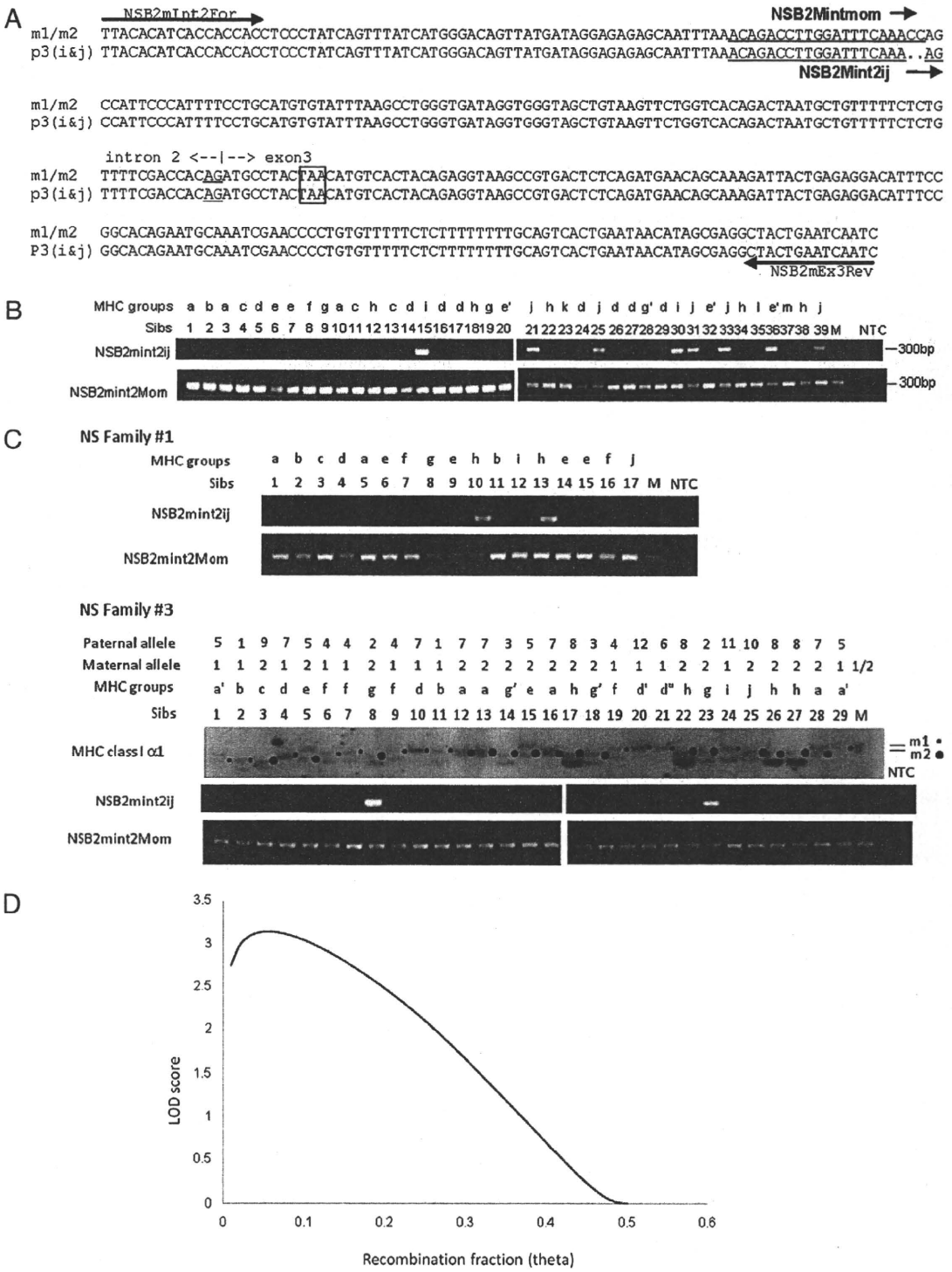

FIGURE 2. The shark *β2M* is linked to the MHC. *A*, The two-nucleotide (CC) deletion polymorphism was found in intron 2 of *β2m* sequences in "*p3*" paternal allele from siblings belonging to the groups "i" and "j." Thus, allele-specific primers were designed based on this polymorphism. All primers are underlined. The ends of coding regions are boxed. The (AG) at the end of intron 2 is underlined. *B*, PCR was carried out with a combination of allele-specific and universal NSB2mEx3Rev reverse primers. Presence or absence of the amplicon using the "*p3*"-specific primers was used for typing (*top gel*) the family 2 with 39 offsprings. Maternal primers were used for the positive control (*bottom gel*). Forward primers are indicated on the *left side* of the gels, and mother and sibling numbers are indicated above the gel along with MHC groups (36). *C*, Allele-specific PCR in the families 1 and 3. Only two animals belonging to the MHC groups "h" possessed the "CC-deletion" allele, and two animals belonging to the "g" groups had this allele in family 3. We partially typed family 3 based on the MHC groups by sequencing of the PBR of the class Ia alleles (maternal and paternal alleles are designated as numbers above the gel) and by Southern blotting with a probe containing MHC class Ia leader and α1 domains (small dot, band for maternal haplotype 1; large dot, maternal haplotype 2). The "*p2*" allele of the "g" group is the only haplotype possessing the "CC-deletion" allele of *β2M*. *D*, Plot of LOD scores at corresponding recombination fractions. The sums of the two families were used (Supplemental Table I).

2*A*), and allele-specific PCR was performed in all members of the nurse shark families in our collection (Fig. 2*B*). Family 1 had two positive members that shared the same paternal MHC haplotype (group "h") (Fig. 2*C*). In family 2, all seven members of groups "i" and "j" bearing the paternal MHC haplotype "*p3*" were positive as well as one other offspring belonging to the "e′" group. Family 3 with 29 offspring, which had not been MHC-typed previously, was tested, and two members were positive for the *β2M* polymorphism (Fig. 2*C*). Typing of this family by Southern blotting as well as sequencing of the class Ia alleles in all offspring showed that these two animals share the same paternal MHC haplotype (Fig. 2*C*). Thus, a total of 11 of 12 siblings positive for the *β2M* polymorphism in three families showed precise cosegregation with certain MHC haplotypes. In addition, 73 of 74 siblings with many other haplotypes lacked this polymorphism, further strongly indicating that *β2M* does not segregate independently of the MHC. The one discordant animal in family 2 (sib 36, group "e′") was also typed by microsatellite analysis and shown to have been sired by the same father as offspring in the "i" and "j" groups; thus this father had the MHC haplotypes "*p3*" and "*p6*" (E.J. Heist et al., submitted for publication), consistent with a paternal intra-MHC recombination event in sib 36. To quantify formally the evidence for linkage of *β2M* to the MHC, we considered all offspring of the two deletion-carrying sires (found within families 2 and 3) as assigned by Southern blotting with class I probes (Fig. 2*C*) (36), sequences of MHC class I alleles (Fig. 2*C*, Table I), and microsatellite analysis (E.J. Heist et al., submitted for publication) (Table I). Family 1 sires have not been microsatellite-characterized, and therefore family 1 was not included in the analysis. We performed a parametric linkage analysis (26) to evaluate the evidence for *β2M* and MHC synteny and obtained a maximum LOD score of 3.14 [1378:1 odds of linkage versus no linkage, equivalent to $p = 7 \times 10^{-5}$ (27)] at a θ of 0.056 (Supplemental Table I, Fig. 2*D*).

β2M *is adjacent to MHC-linked* Ring3

Ring3 (or *BRD2*) is a putative nuclear transcriptional regulator and a nuclear kinase required for early development (38–41) with no defined immune functions but nevertheless linked to the MHC of all other gnathostomes and to the "proto-MHC" in lower deuterostomes (42). A portion of *ring3* was initially cloned via degenerate PCR from nurse shark spleen cDNA, and this short fragment was used as a probe to isolate a full-length cDNA from a phage library. BLAST searches and phylogenetic tree analysis confirmed the orthology of nurse shark *ring3* to that of other species (GenBank accession number HM625830) (Fig. 3*A*). The nurse shark *ring3* is ubiquitously expressed (Fig. 1*B*). To ensure that the shark *ring3* is linked to the MHC as in all other species examined (8), we performed ssCP analysis using siblings of family 2 (Fig. 3*B*). Two distinguishing *ring3* bands corresponding with the maternal MHC allele *m2* were found in those siblings possessing this allele (groups "i" and "d" in Fig. 3) with 100% fidelity, demonstrating that *ring3* is closely linked to the MHC and further confirming the *β2M* linkage. We identified other BAC clones that were either *β2M*- or *ring3*-single-positive; unfortunately, none of them was positive for other MHC genes, again consistent with larger intergenic distances in sharks compared with those of other species (36). Chen et al. (29) drew a premature conclusion of non-MHC linkage; however, determining the linkage status of *β2M* (or almost any gene) based on a single BAC sequence is not sufficient for the shark genome, where there are large intragenic and intergenic distances. Several nurse shark BAC clones (22) were isolated with the *ring3* and *β2M* probes, and some of them were positive for both genes. As previously reported (29), the *β2M* gene contains at least three exons, having a similar genomic organization and size to other species. The shark *ring3* gene spans ~20 kb and contains 12 exons, which is approximately twice as large as mammalian *ring3* genes (e.g., 12.8 kb and 9.7 kb for human and mouse, respectively), consistent with a larger gene size found in most shark MHC genes (36). Sequencing through an entire BAC clone (GC_614H19) confirmed that the *β2M* and *ring3* genes were adjacent to each other ~45 kb apart (Fig. 4).

Genetic descent of β2M

The chromosomal location of the *β2M* gene varies greatly among vertebrate species (Fig. 5). Genomic synteny is well conserved in

Table I. List of sibs used for statistical analysis

	MHC[a]		Haplotypes		m-Satellite	Phase	
Sib No.	Old Group	New Group	MHC Class Ia	β2m	Sire	1	2
Family 2							
15	i	i	m2/p3	del	4	NR	R
30	i	i	m2/p3	del	4	NR	R
21	j	j	m1/p3	del	4	NR	R
25	j	j	m1/p3	del	4	NR	R
31	j	j	m1/p3	del	4	NR	R
33	j	j	m1/p3	del	4	NR	R
39	j	j	m1/p3	del	4	NR	R
20	e′	e′	m1/p6	ins	4	NR	R
32	e′	e′	m1/p6	ins	4	NR	R
36	e′	e′	m1/p6	del	4	R	NR
28	g′	g′	m2/p6[b]	ins	4	NR	R
13	c	g′	m2/p6[b]	ins	4	NR	R
Family 3							
8		g	m2/p2	del	2	NR	R
23		g	m2/p2	del	2	NR	R
6		d	m1/p4	ins	2	NR	R
7		d	m1/p4	ins	2	NR	R
9		d	m1/p4	ins	2	NR	R
19		d	m1/p4	ins	2	NR	R

[a]Old group is taken from Ref. 28, and new groups are assigned in this study.
[b]MHC class Ia sequences revealed that sib 13 is further categorized with group g′ in this study.
del, CC-deletion haplotype; NR, nonrecombinant; R, recombinant.

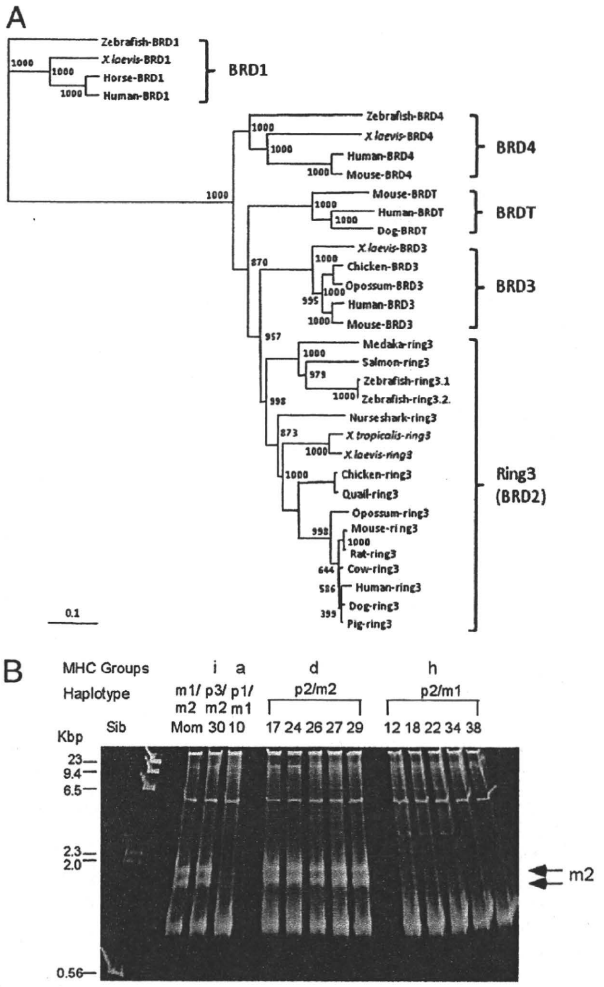

FIGURE 3. *A*, Phylogenetic tree analysis of Ring3 and homologues. GenBank accession numbers used in this analysis are as follows. Ring3 (BRD2): CAM25760 (human), AAY34703 (bovine), CAI11405 (dog), CAA15819 (mouse), CAE83937 (rat), XP_001369391 (opossum), CAN13285 (pig), CAA65449 (chicken), BAC82511 (quail), AAI68574 (*X. tropicalis*), AAI30180 (*X. laevis*), CAK04960 (zebrafish-1), CAD54663 (zebrafish-2), ABQ59684 (salmon), BAD93258 (medaka). Additional accession numbers for Ring3 homologues used for this analysis are the following: BRD3: AAI29055 (*X. laevis*), NP_031397 (human), NP_075825 (mouse), XP_001365890 (opossum), XP_425330 (Chicken). BRDT: NP_473395 (mouse), NP_997072 (human), XP_537079 (dog). BRD4: NP_490597 (human), NP_065254 (mouse), NP_001104751 (zebrafish), AAH76786 (*X. laevis*). BRD1: NP_001157300 (horse), XP_698063 (zebrafish), NP_001085846 (*X. laevis*), CAG30294 (human). Gene names are noted after species name. BRD1 does not map to an MHC paralogous region, whereas BRDT, BRD3, and BRD4 are found in the MHC paralogous regions. The tree was constructed using the NJ method, rooted with BRD1, and bootstrapping analysis was done with 1000 runs. Values are noted at the branch nodes, and an asterisk (*) indicates no significant value. The scale indicates the divergence time. *B*, The shark *ring3* maps to the MHC. Primers from exons 4 and 5 were used for PCR amplification and ssCP analysis. The ~1440-bp amplicon from the siblings along with mother shark genomic DNA were loaded on an 0.5× MDE gel. Under these conditions, "*m2*" was identified as two distinctive bands indicated as arrows. Mother and sibling numbers are indicated above the gel along with MHC groups and haplotype combinations from previous work (36).

the region of chicken *β2M* relative to humans except for deletions of certain genes (43), and the same seems to be true for the *Anolis* lizard in which the synteny near the *β2M* gene (GenBank accession number FG703784, etc.) is conserved (genomic scaffold-670, 634,364 bp) (Supplemental Table II). Mouse *β2M* is linked to the so-called minor histocompatibility complex on chromosome 2 (16) and is located within a small region syntenic to human chromosome 15 (43). Notably, a smaller syntenic block is embedded with genes mapping to human chromosome 14q11.2 in a marsupial, the opossum. Although these regions can be accounted for by block translocations or syntenic breakpoints, synteny is not conserved in species from lower vertebrate classes as *β2M* is surrounded by genes mapping to various human chromosomes. The amphibian *Xenopus β2M* is linked to the genes mapping to human chromosomes 16 and 17 (genomic scaffold-673). In zebrafish, *β2M* (chromosome 4) is surrounded by genes mapping to human chromosome 12p12, and various locations in the human genome have syntenic regions on the *Fugu* scaffold-171 (638,182 bp). As mentioned above, the teleost fish experienced a recent genome-wide duplication ("3R"), and there is another *β2M* locus in the zebrafish genome that is ~60% similar to its paralogue at the amino acid level. Notably, the second *β2M* locus is found at the telomeric region of chromosome 8 and is distantly linked to a class IIA gene and two class Ib genes of the L-lineage (44) (Supplemental Table II). Although the *β2M* linkage is not very close (i.e., 6.5 Mbp apart) in this chromosomal region (considering the rapid reorganization of syntenic regions in the teleost fish), this linkage group of class II/class I/*β2M* is likely a vestige of the primordial synteny. Combining all of the evidence, our study in nurse shark demonstrates that *β2M* was originally encoded in the MHC, and from extensive database analysis in many taxa, this gene underwent multiple translocations in gnathostomes, either stepwise or independently from the MHC (Fig. 5).

Discussion

Compared with other vertebrate models (e.g., chicken or teleost fish), the shark genome seems to be stable, first demonstrated with the linkage of MHC class I and II genes (21), which was lost in bony fish (28), and later with linkage conservation of genes found in the mammalian MHC class III region (37). These MHC linkage data are consistent with global genomic studies in the elephant shark suggesting that cartilaginous fish have greater preservation of synteny than is found in any teleost model (45, 46). The *β2M* linkage to the shark MHC demonstrated here is likely the primordial condition, thus further supporting the conservation of the cartilaginous fish genome. Furthermore, the close proximity of class I, class II, and *β2M* is consistent with the theory that they were derived from a common ancestor by tandem (*cis*) duplication. The close linkage of *β2M* and class I may have regulated their original coordinated expression and upregulation. Class I and *β2M* expression is nearly identical in the nurse shark (Fig. 1*B*), but in other vertebrates β2M is made in excess (47). Furthermore, the number of *β2M* loci is expanded in rainbow trout (48) and polyploid *Xenopus* species (18).

Unlike class II genes, class I genes are extraordinarily plastic. Besides the MHC-linked classical class Ia genes, there are also many nonclassical class Ib genes with varied functions, some encoded in the MHC and others not. The majority of class Ib proteins associates with β2M as well, and it has been speculated that there was an advantage of translocation of *β2M* out of the MHC so that it would not be subject to duplications and deletions (19), like class I genes in many vertebrates. Consistent with the idea of maintaining genomic stability, but in contrast to class I and class II genes, both *β2M* and *ring3* genes are in a very stable part of the shark MHC, with very few polymorphisms and transposable elements (Fig. 4); there was no polymorphism detected by using restriction enzymes/Southern blotting with either the *ring3* or *β2M* probe. Although there are a few bony fish species in which

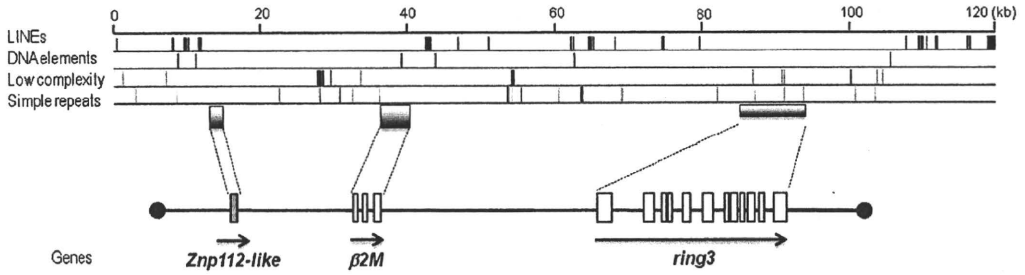

FIGURE 4. Map of BAC clone GC_614H19. Gene orientation is indicated as arrows and exons are shown in boxes. Only one exon for *ZFP112-like* gene was identified based on the similarity to other species. The positions of repetitive elements are shown above the map classified into four different categories. The total interspersed repeats are found in ~5.35% of the sequences, consisting of ~4.74% of LINEs and ~0.63% of simple repeats. Each exon is indicated as a box, and transcriptional orientations are shown with an arrow in the 5′ to 3′ direction. The sequence has been deposited in the DNA Data Bank of Japan under accession number AB571627.

the number of *β2M* loci has been expanded (49), and there are two loci in the tetraploid *Xenopus laevis* (18), generally these species are exceptions. There seems to be only one *β2M* locus in the nurse shark genome, because genomic Southern blotting with many restriction enzymes yielded a single band with an exon-specific probe (Fig. 1*C*).

The primordial linkage of *β2M* to the MHC does not contribute to the debate on which gene came first, class I or class II. Among the various IgSF domains, the C1-type is a rare form, found primarily in molecules associated with adaptive immunity (50). Therefore, it is reasonable to propose that C1-type IgSF-encoding genes like *β2M* were present in the "proto-MHC," which then acquired the PBR from another gene family. Furthermore, it has been speculated that all molecules containing C1-type IgSF domains arose from a common ancestor, and thus an Ig/TCR precursor may have originated from the "proto-MHC" (20). Consistent with previous studies dating back almost 30 y (3, 5, 33, 34), our phylogenetic analysis demonstrated a common origin for the class IIA/*DMB*/*β2M* and the class Ia/*DMA*/class IIB lineages, and all of these genes share an ancestral C1 domain-encoding exon that emerged after the split between Ag receptors and MHC genes (Fig. 1*B*). Whereas *class IIA*, *β2M*, *class IIB*, and *class Ia* share an immediate common ancestor that arose by tandem duplication from the ancestral molecule, each *DM* gene was apparently generated by tandem duplications of class IIA and class IIB, perhaps early after the emergence of tetrapods, as no *DM* genes have been found in the teleost or cartilaginous fish; the maximum likelihood and Bayesian inference trees favor this scenario (S2). The NJ tree (Fig. 1*B*), however, suggests that shark class IIA and IIB genes cluster with class II genes from other species rather than at the basal position of class II/*DM*, suggesting that sharks may indeed possess *DM*.

An orthologous gene related to the ancestor of *ring3* is present in the urochordate (e.g., amphioxus) "proto-MHC" (42), and thus the MHC-linkage of *ring3* in sharks is not surprising. To determine the linkage status in other cartilaginous fish species, we examined the elephant shark genome. Current analyses of the elephant shark genome (46) has yielded only short (<1 kbp) scaffolds (AAVX01540028.1) in which we only identified the *β2M* C1 domain. Three scaffolds were found to contain some exons of the elephant shark *ring3* gene [AAVX01538535 (754 bp), AAVX01069837 (5232 bp), AAVX01012433 (4324 bp)]; however, the assembly is still in its early stages. Further progress in this genome project will reveal the synteny around *β2M* and all of the other MHC genes and likely provide insight into the natural history of the adaptive immune system by revealing other genes that have been translocated out of the MHC during vertebrate evolution. For example, there is good evidence from various vertebrates that both IgSF- and C-type lectin-containing NK cell receptor genes (in humans, they are encoded in leukocyte receptor complex and NK complex, respectively) and the

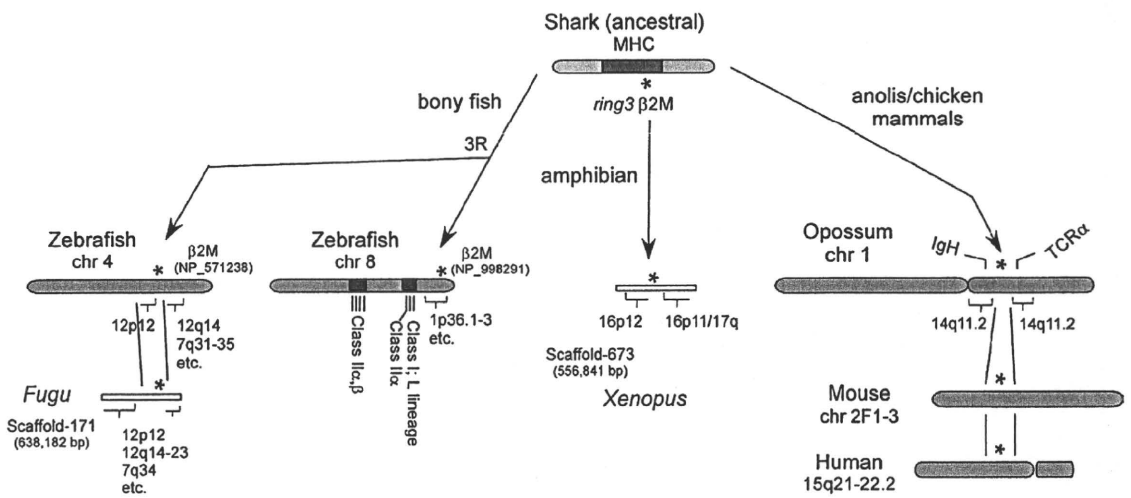

FIGURE 5. Inconsistent synteny of *β2M* among vertebrate species. Genomic synteny of *β2M* is not consistent in bony fish and *Xenopus*, suggesting that multiple translocations of *β2M* occurred over evolutionary time. An asterisk (*) indicates the location of the *β2M* gene, and brackets indicate the genomic regions corresponding with the particular human chromosome. The detailed gene assignments can be obtained in Supplemental Table II. IgH and TCRα loci are marked in opossum chromosome 1.

MHC were genetically linked at an early point in vertebrate evolution (20, 51, 52), suggesting that NK receptors co-evolved with MHC proteins. We have found a fragment of a zinc finger protein (ZFP), ZFP112-like, in BAC clone GC_614H19, adjacent to *β2M* (Fig. 5). *ZFP112* is found on human chromosome 19q13.2 near *FcRn* (19q13.3), a nonclassical class Ib molecule, and the leukocyte receptor complex (19q13.4). This region had been suggested to be an MHC paralogous region by pericentric inversion of 19p13.1. Whether the nurse shark *ZNF112* is a pseudogene or divergent from human/rodent *ZFP112* genes, the linkage of *ZFP112* suggests that the linkage of NK receptor(s) and MHC could be preserved in the shark genome. Furthermore, we found *β2M* on the same chromosome as *TCRα/δ* in horse (chromosome 1), cow (chromosome 10), and both *TCRα/δ* and *Ig* in the opossum genome (Fig. 5, Supplemental Table II). In addition, Ag receptor loci and other genes involved in immune defense (e.g., B7 ligands and Fc-like receptors) are linked to genes related to the *Xenopus* MHC (Y. Ohta and M.F. Flajnik, manuscripts in preparation), and cathepsins S and L are found on MHC paralogous regions in mammals (20). Such evidence is consistent with our hypothesis that Ag receptors (*TCR, Ig*), NK receptors, and other genes involved in Ag processing and generally in immune function might have been linked in a "pre-adaptive immune complex" in the ancestral configuration.

Acknowledgments

We thank Dr. Mike Criscitiello and Caitlin Doremus for critical reading.

Disclosures

The authors have no financial conflicts of interest.

References

1. Flajnik, M. F., and L. Du Pasquier. 2008. Evolution of the immune system. In *Fundamental Immunology.* W. E. Paul, ed. Lippincott Williams & Wilkins, Philadelphia, p. 56–124.
2. Flajnik, M. F., C. Canel, J. Kramer, and M. Kasahara. 1991. Which came first, MHC class I or class II? *Immunogenetics* 33: 295–300.
3. Kaufman, J. F., and J. L. Strominger. 1982. HLA-DR light chain has a polymorphic N-terminal region and a conserved immunoglobulin-like C-terminal region. *Nature* 297: 694–697.
4. Klein, J., and C. O'hUigin. 1993. Composite origin of major histocompatibility complex genes. *Curr. Opin. Genet. Dev.* 3: 923–930.
5. Hughes, A. L., and M. Nei. 1993. Evolutionary relationships of the classes of major histocompatibility complex genes. *Immunogenetics* 37: 337–346.
6. Meyer, A., and Y. Van de Peer. 2005. From 2R to 3R: evidence for a fish-specific genome duplication (FSGD). *Bioessays* 27: 937–945.
7. Postlethwait, J., A. Amores, W. Cresko, A. Singer, and Y. L. Yan. 2004. Subfunction partitioning, the teleost radiation and the annotation of the human genome. *Trends Genet.* 20: 481–490.
8. Flajnik, M. F., and M. Kasahara. 2001. Comparative genomics of the MHC: glimpses into the evolution of the adaptive immune system. *Immunity* 15: 351–362.
9. Nonaka, M., C. Namikawa, Y. Kato, M. Sasaki, L. Salter-Cid, and M. F. Flajnik. 1997. Major histocompatibility complex gene mapping in the amphibian *Xenopus* implies a primordial organization. *Proc. Natl. Acad. Sci. USA* 94: 5789–5791.
10. Kaufman, J., S. Milne, T. W. Göbel, B. A. Walker, J. P. Jacob, C. Auffray, R. Zoorob, and S. Beck. 1999. The chicken B locus is a minimal essential major histocompatibility complex. *Nature* 401: 923–925.
11. Clark, M. S., L. Shaw, A. Kelly, P. Snell, and G. Elgar. 2001. Characterization of the MHC class I region of the Japanese pufferfish (*Fugu* rubripes). *Immunogenetics* 52: 174–185.
12. Matsuo, M. Y., S. Asakawa, N. Shimizu, H. Kimura, and M. Nonaka. 2002. Nucleotide sequence of the MHC class I genomic region of a teleost, the medaka (*Oryzias latipes*). *Immunogenetics* 53: 930–940.
13. Michalová, V., B. W. Murray, H. Sültmann, and J. Klein. 2000. A contig map of the Mhc class I genomic region in the zebrafish reveals ancient synteny. *J. Immunol.* 164: 5296–5305.
14. Phillips, R. B., A. Zimmerman, M. A. Noakes, Y. Palti, M. R. Morasch, L. Eiben, S. S. Ristow, G. H. Thorgaard, and J. D. Hansen. 2003. Physical and genetic mapping of the rainbow trout major histocompatibility regions: evidence for duplication of the class I region. *Immunogenetics* 55: 561–569.
15. Shiina, T., J. M. Dijkstra, S. Shimizu, A. Watanabe, K. Yanagiya, I. Kiryu, A. Fujiwara, C. Nishida-Umehara, Y. Kaba, I. Hirono, et al. 2005. Interchromosomal duplication of major histocompatibility complex class I regions in rainbow trout (Oncorhynchus mykiss), a species with a presumably recent tetraploid ancestry. *Immunogenetics* 56: 878–893.
16. Michaelson, J. 1981. Genetic polymorphism of beta 2-microglobulin (B2m) maps to the H-3 region of chromosome 2. *Immunogenetics* 13: 167–171.
17. Riegert, P., R. Andersen, N. Bumstead, C. Döhring, M. Dominguez-Steglich, J. Engberg, J. Salomonsen, M. Schmid, J. Schwager, K. Skjødt, and J. Kaufman. 1996. The chicken beta 2-microglobulin gene is located on a non-major histocompatibility complex microchromosome: a small, G+C-rich gene with X and Y boxes in the promoter. *Proc. Natl. Acad. Sci. USA* 93: 1243–1248.
18. Stewart, R., Y. Ohta, R. R. Minter, T. Gibbons, T. L. Horton, P. Ritchie, J. D. Horton, M. F. Flajnik, and M. D. Watson. 2005. Cloning and characterization of *Xenopus* beta2-microglobulin. *Dev. Comp. Immunol.* 29: 723–732.
19. Ono, H., F. Figueroa, C. O'hUigin, and J. Klein. 1993. Cloning of the beta 2-microglobulin gene in the zebrafish. *Immunogenetics* 38: 1–10.
20. Flajnik, M. F., and M. Kasahara. 2010. Origin and evolution of the adaptive immune system: genetic events and selective pressures. *Nat. Rev. Genet.* 11: 47–59.
21. Ohta, Y., K. Okamura, E. C. McKinney, S. Bartl, K. Hashimoto, and M. F. Flajnik. 2000. Primitive synteny of vertebrate major histocompatibility complex class I and class II genes. *Proc. Natl. Acad. Sci. USA* 97: 4712–4717.
22. Luo, M., H. Kim, D. Kudrna, N. B. Sisneros, S. J. Lee, C. Mueller, K. Collura, A. Zuccolo, E. B. Buckingham, S. M. Grim, et al. 2006. Construction of a nurse shark (Ginglymostoma cirratum) bacterial artificial chromosome (BAC) library and a preliminary genome survey. *BMC Genomics* 7: 106.
23. Bartl, S., M. A. Baish, M. F. Flajnik, and Y. Ohta. 1997. Identification of class I genes in cartilaginous fish, the most ancient group of vertebrates displaying an adaptive immune response. *J. Immunol.* 159: 6097–6104.
24. Saitou, N., and M. Nei. 1987. The neighbor-joining method: a new method for reconstructing phylogenetic trees. *Mol. Biol. Evol.* 4: 406–425.
25. Page, R. D. 1996. TreeView: an application to display phylogenetic trees on personal computers. *Comput. Appl. Biosci.* 12: 357–358.
26. Ott, J. 1999. *Analysis of Human Genetic Linkage.* The Johns Hopkins University Press, Baltimore, MD.
27. Lander, E., and L. Kruglyak. 1995. Genetic dissection of complex traits: guidelines for interpreting and reporting linkage results. *Nat. Genet.* 11: 241–247.
28. Sato, A., F. Figueroa, B. W. Murray, E. Málaga-Trillo, Z. Zaleska-Rutczynska, H. Sültmann, S. Toyosawa, C. Wedekind, N. Steck, and J. Klein. 2000. Nonlinkage of major histocompatibility complex class I and class II loci in bony fishes. *Immunogenetics* 51: 108–116.
29. Chen, H., S. Kshirsagar, I. Jensen, K. Lau, C. Simonson, and S. F. Schluter. 2010. Characterization of arrangement and expression of the beta-2 microglobulin locus in the sandbar and nurse shark. *Dev. Comp. Immunol.* 34: 189–195.
30. Williams, A. F., and A. N. Barclay. 1988. The immunoglobulin superfamily—domains for cell surface recognition. *Annu. Rev. Immunol.* 6: 381–405.
31. Saper, M. A., P. J. Bjorkman, and D. C. Wiley. 1991. Refined structure of the human histocompatibility antigen HLA-A2 at 2.6 A resolution. *J. Mol. Biol.* 219: 277–319.
32. Criscitiello, M. F., R. Benedetto, A. Antao, M. R. Wilson, V. G. Chinchar, N. W. Miller, L. W. Clem, and T. J. McConnell. 1998. Beta 2-microglobulin of ictalurid catfishes. *Immunogenetics* 48: 339–343.
33. Flajnik, M. F., K. Miller, and P. L. Du. 2003. Evolution of the immune system. In *Fundamental Immunology.* W. E. Paul, ed. Lippincott Williams & Wilkins, Philadelphia, p. 519–570.
34. O'hUigin, C., H. Sültmann, H. Tichy, and B. W. Murray. 1998. Isolation of mhc class II DMA and DMB cDNA sequences in a marsupial: the gray short-tailed opossum (Monodelphis domestica). *J. Mol. Evol.* 47: 578–585.
35. Kasahara, M., C. Canel, E. C. McKinney, and M. F. Flajnik. 1991. Molecular cloning of nurse shark cDNAs with high sequence similarity to nucleoside diphosphate kinase genes. In *Evolution of the Major Histocompatibility Complex.* J. Klein, ed. Springer-Verlag, New York, p. 491–499.
36. Ohta, Y., E. C. McKinney, M. F. Criscitiello, and M. F. Flajnik. 2002. Proteasome, transporter associated with antigen processing, and class I genes in the nurse shark Ginglymostoma cirratum: evidence for a stable class I region and MHC haplotype lineages. *J. Immunol.* 168: 771–781.
37. Terado, T., K. Okamura, Y. Ohta, D. H. Shin, S. L. Smith, K. Hashimoto, T. Takemoto, M. I. Nonaka, H. Kimura, M. F. Flajnik, and M. Nonaka. 2003. Molecular cloning of C4 gene and identification of the class III complement region in the shark MHC. *J. Immunol.* 171: 2461–2466.
38. Denis, G. V., M. E. McComb, D. V. Faller, A. Sinha, P. B. Romesser, and C. E. Costello. 2006. Identification of transcription complexes that contain the double bromodomain protein Brd2 and chromatin remodeling machines. *J. Proteome Res.* 5: 502–511.
39. Sinha, A., D. V. Faller, and G. V. Denis. 2005. Bromodomain analysis of Brd2-dependent transcriptional activation of cyclin A. *Biochem. J.* 387: 257–269.
40. Denis, G. V., C. Vaziri, N. Guo, and D. V. Faller. 2000. RING3 kinase transactivates promoters of cell cycle regulatory genes through E2F. *Cell Growth Differ.* 11: 417–424.
41. Denis, G. V., and M. R. Green. 1996. A novel, mitogen-activated nuclear kinase is related to a Drosophila developmental regulator. *Genes Dev.* 10: 261–271.
42. Danchin, E. G., and P. Pontarotti. 2004. Towards the reconstruction of the bilaterian ancestral pre-MHC region. *Trends Genet.* 20: 587–591.
43. Jones, C. T., D. R. Morrice, I. R. Paton, and D. W. Burt. 1997. Gene homologs on human chromosome 15q21-q26 and a chicken microchromosome identify a new conserved segment. *Mamm. Genome* 8: 436–440.
44. Dijkstra, J. M., T. Katagiri, K. Hosomichi, K. Yanagiya, H. Inoko, M. Ototake, T. Aoki, K. Hashimoto, and T. Shiina. 2007. A third broad lineage of major histocompatibility complex (MHC) class I in teleost fish; MHC class II linkage and processed genes. *Immunogenetics* 59: 305–321.

45. Kulski, J. K., T. Shiina, T. Anzai, S. Kohara, and H. Inoko. 2002. Comparative genomic analysis of the MHC: the evolution of class I duplication blocks, diversity and complexity from shark to man. *Immunol. Rev.* 190: 95–122.
46. Venkatesh, B., E. F. Kirkness, Y. H. Loh, A. L. Halpern, A. P. Lee, J. Johnson, N. Dandona, L. D. Viswanathan, A. Tay, J. C. Venter, et al. 2007. Survey sequencing and comparative analysis of the elephant shark (Callorhinchus milii) genome. *PLoS Biol.* 5: e101.
47. Ploegh, H. L., L. E. Cannon, and J. L. Strominger. 1979. Cell-free translation of the mRNAs for the heavy and light chains of HLA-A and HLA-B antigens. *Proc. Natl. Acad. Sci. USA* 76: 2273–2277.
48. Magor, K. E., B. P. Shum, and P. Parham. 2004. The beta 2-microglobulin locus of rainbow trout (Oncorhynchus mykiss) contains three polymorphic genes. *J. Immunol.* 172: 3635–3643.
49. Shum, B. P., K. Azumi, S. Zhang, S. R. Kehrer, R. L. Raison, H. W. Detrich, and P. Parham. 1996. Unexpected beta2-microglobulin sequence diversity in individual rainbow trout. *Proc. Natl. Acad. Sci. USA* 93: 2779–2784.
50. Du Pasquier, L. 2000. Relationships among the genes encoding MHC molecules and the specific antigen receptors. In *MHC Evolution, Structure and Function.* L. Du Pasquier, and M. Kasahawa, eds. Springer-Verlag, Tokyo, p. 53–65.
51. Rogers, S. L., T. W. Göbel, B. C. Viertlboeck, S. Milne, S. Beck, and J. Kaufman. 2005. Characterization of the chicken C-type lectin-like receptors B-NK and B-lec suggests that the NK complex and the MHC share a common ancestral region. *J. Immunol.* 174: 3475–3483.
52. Trowsdale, J. 2001. Genetic and functional relationships between MHC and NK receptor genes. *Immunity* 15: 363–374.

doi: 10.1111/j.1365-3083.2011.02524.x

NFKBIL1 Confers Resistance to Experimental Autoimmune Arthritis Through the Regulation of Dendritic Cell Functions

T. Chiba*[1], Y. Matsuzaka†[1], T. Warita†, T. Sugoh*, K. Miyashita*, A. Tajima†, M. Nakamura‡, H. Inoko†, T. Sato* & M. Kimura†

*Departments of Immunology, †Molecular Life Science, and ‡Pathology, Tokai University School of Medicine, Kanagawa, Japan

Received 14 October 2010; Accepted in revised form 13 January 2011

Correspondence to: T. Sato, Department of Immunology, Tokai University School of Medicine, Shimokasuya 143, Isehara, Kanagawa 259-1193, Japan. E-mail: takehito@is.icc.u-tokai.ac.jp

[1]These authors contributed equally.

Abstract

We and others have reported that human NF-κB inhibitor-like-1 (NFKBIL1) was a putative susceptible gene for autoimmune diseases such as rheumatoid arthritis (RA). However, its precise role in the pathogenesis of RA is still largely unknown. In this study, we generated transgenic mice expressing human NFKBIL1 (NFKBIL1-Tg) and examined whether NFKBIL1 plays some role(s) in the development of autoimmune arthritis. In both a collagen-induced arthritis model and a collagen antibody-induced arthritis model, NFKBIL1-Tg mice showed resistance to arthritis compared to control mice, indicating that the gene product of NFKBIL1 was involved in the control of thusly induced arthritis. Total spleen cells of NFKBIL1-Tg mouse showed decreased proliferation to mitogenic stimuli, consistent with its resistance to arthritis. Unexpectedly, purified T cells of NFKBIL1-Tg mouse showed increased proliferation and cytokine production. This apparent discrepancy was accounted for by the impaired functions of antigen-presenting cells of NFKBIL1-Tg mouse; both T/B cell-depleted spleen cells and bone marrow-derived dendritic cells of the Tg mouse induced less prominent proliferation and IL-2 production of T cells. Furthermore, dendritic cells (DCs) derived from NFKBIL1-Tg mouse showed lower expression of co-stimulatory molecules and decreased production of inflammatory cytokines when they were activated by lipopolysaccharide. Taken together, these results indicated that NFKBIL1 affected the pathogenesis of RA at least in part through the regulation of DC functions.

Introduction

Rheumatoid arthritis (RA) is a chronic inflammatory and joint-destroying autoimmune disease and is one of the most serious issues in the field of medicine [1]. Antigen-presenting cells (APC) such as dendritic cells (DCs) play pivotal roles for pathological setting of RA. Indeed, adoptive transfer of type II collagen-pulsed DCs is sufficient for the induction of autoimmune arthritis [2]. DCs provide cognate interaction, which is crucial for successful activation of T cells. Furthermore, DCs are main cellular source of inflammatory cytokines such as IL-6 and TNFα. As dysregulation of transcription factor nuclear factor κB (NF-κB) activity induces excessive production of inflammatory cytokines, leading to systemic and local autoimmune disorders such as systemic lupus erythematosus (SLE) and RA, the control of NF-κB seems essential for preventing such diseases [3–5].

Genetic polymorphisms are known to affect RA pathogenesis [6]. We and others revealed that single nucleotide polymorphism (SNP) in the promoter region of NFKBIL1 was associated with the pathogenesis of RA [7, 8]. NKBILL1 gene is located within the MHC class III region and encodes NFKBIL1 protein also known as IκBL. NFKBIL1 has been well conserved throughout evolution (more than 90% identical amino acids between human and mouse) and contains the ankyrin repeat domain, which exhibits high homology with the IκB family protein, suggesting that NFKBIL1 can modulate NF-κB activity, but its precise role and contribution to RA development are still to be unravelled [9, 10].

SCANDINAVIAN JOURNAL OF immunology AN INTERNATIONAL MONTHLY JOURNAL

There are several experimental animal models of human autoimmune disease. As for RA, collagen-induced arthritis (CIA) and collagen antibody-induced arthritis (CAIA) are widely used for the evaluation of responsible genes. In this study, we generated NFKBIL1-Tg mice and found that they showed significant resistance to both CIA and CAIA. In addition, we demonstrated the impaired function of DCs in the Tg mice. These findings suggested that NFKBIL1 was involved in the control of RA pathogenesis via the regulation of innate immune cell functions.

Materials and methods

Generation of NFKBIL1-Tg mice. Human NFKBIL1 cDNA (BC143671) was cloned into pDRIVE-CAG vector (InvivoGen, San Diego, CA, USA), which contains CAG promoter combined with human cytomegalovirus immediate-early enhancer and a modified chicken β-actin promoter with the first intron. This construct was used as a transgene. NFKBIL1-Tg mice were generated by pronucleus microinjection into BDF1 × C57BL/6 fertilized eggs. Progeny mice were crossed with DBA/1j mice (Clea Japan, Inc., Tokyo, Japan) and germline transmission of NFKBIL1 transgene was confirmed by genomic PCR with specific primers (sense, 5′-ATGAGTAACCCC-TCCCCCCAG-3′; antisense, 5′-CACATCACCAAATCG-CCAGA-3′). Then, the mice expressing NFKBIL1 were backcrossed with DBA/1j mice over eight generations. All animals were bred in specific pathogen-free condition and used at 4–12 weeks of age. All mouse experiments were approved by the Animal Experimentation Committee, Isehara campus (Tokai University, Kanagawa, Japan).

Antibodies and reagents. Fluorescein isothiocyanate (FITC)-conjugated anti-CD19 (1D3), FITC-conjugated anti-CD44 (IM7), PerCP-Cy5.5-conjugated anti-CD4 antibody (RM4-5) and APC-conjugated anti-CD11c antibody (HL3) were purchased from BD Biosciences (Franklin Lakes, NJ, USA). FITC-conjugated anti-CD80 (16-10A1) and FITC-conjugated Thy1.2 (53-2.1), PE-labelled anti-CD25 (PC61.5), PE-labelled anti-CD86 (PO.3), APC-labelled anti-CD8 (53-6.7), APC-labelled anti-IL-2 (JES6-5H4) and purified anti-CD28 antibody (37.51) were purchased from eBioscience (San Diego, CA, USA). Anti-mouse CD3ε antibody (145-2C11) was prepared in our laboratory. Concanavalin A (ConA) (C5275), phorbol 12-myristate 13-acetate (PMA) (P1585), ionomycin (I0634) and brefeldin A (BFA) (B6542) were purchased from Sigma-Aldrich (St Louis, MO, USA). Lipopolysaccharide (LPS) for DC stimulation was purchased from Santa Cruz Biotechnology (sc-3535; Santa Cruz, CA, USA).

Collagen-induced arthritis and collagen antibody-induced arthritis. NFKBIL1-Tg mice and littermate control mice with DBA/1j background were immunized with 200 μg of chicken type II collagen (CII; Chondrex, Seattle, WA, USA) emulsified with complete Freund's adjuvant (CFA; Chondrex) intradermally at the base of the tail on day 0. Three weeks later, mice were immunized again with CII without CFA. Mice were examined for up to 100 days. Clinical signs of arthritis were assessed daily and graded: 0, no swelling; 1, paw with single joint; 2, paw with two joints; 3, paw with multiple joints; 4, severe swelling and joint rigidity. Each limb was graded, giving a maximum possible score of 12 per mouse. For CAIA induction, a mixture of anti-CII monoclonal antibodies (2 mg/500 μl; Chondrex) was administered intraperitoneally on day 0. Three days later, LPS (50 μg/100 μl; Chondrex) was injected intraperitoneally. Clinical signs were assessed daily and graded similarly to CIA, with brief modification.

Joint histology. Joints were fixed in 10% formaldehyde and decalcified with 5% formic acid. Fixed joints were embedded in paraffin, sectioned into 4 μm thickness, stained with haematoxylin and eosin, and examined for collagen disruption, pannus formation, synovial space infiltrates and cartilage/bone erosion.

Cell isolation and culture. All cells used in this study were maintained in RPMI1640 medium supplemented with 10%FCS, 2 mM L-glutamine, 50 mM 2-ME, 100 U/ml penicillin, 100 μg/ml streptomycin and 1 mM sodium pyruvate. Spleen $CD4^+$ T cells were isolated by using mouse CD4 dynabeads and Detacha CD4 according to the manufacturer's instructions (Invitrogen/Dynal; Carlsbad, CA, USA). For naïve and memory-phenotype T cell preparation, enriched $CD4^+$ cells were incubated with FITC-labelled anti-CD44 antibody plus PE-labelled anti-CD25 and fractionated by FACSAria (BD Biosciences) according to the CD44/CD25 expressions. Spleen $CD8^+$ T cells were isolated by AutoMACS system (Miltenyi Biotec; Bergisch Gladbach, Germany) after staining with anti-CD8 and anti-rat IgG MACS beads. $CD4^+$ cell-depleted spleen cells were incubated with FITC-labelled anti-Thy1.2 and CD19, and then, the $Thy1.2^-$, $CD19^-$ fraction was purified by FACSAria and used as non-T and non-B cells. Bone marrow cells were cultured in 10%FCS/RPMI with 5 ng/ml granulocyte-macrophage colony-stimulating factor (GM-CSF, AF-315-03; PeproTech, Rocky Hill, NJ, USA). Half of the culture medium was replaced by fresh 5 ng/ml GM-CSF in 10%FCS/RPMI after 3 days. Cells were used at 10 or 11 days of culture as bone marrow-derived dendritic cells (BMDC). In some cases, $CD4^+$ T cells were cultured with APC at a ratio of 10:1 in the presence of 10 μg/ml anti-CD3ε antibody. Splenic $CD11c^+$ cells were isolated by using mouse Pan DC microbeads according to manufacturer's procedure (Miltenyi Biotec).

{^{3}H}-thymidine incorporation. Whole splenocytes, $CD4^+$ T cells, $CD8^+$ T cells, $CD4^+$ naïve T cells and memory-phenotype T cells were cultured in 96-well plates for 48–

72 h, with 1 μCi [^{3}H]-thymidine added to each well for the last 18 h. Cells were harvested and [^{3}H]-thymidine uptake was measured by scintillation counter.

Measurement of cytokine production. The amounts of mouse IL-1β, IL-6, IL-12p70 and TNFα in culture supernatants were measured by flow cytometric beads array (CBA; BD Biosciences) according to manufacturer's instructions. The data were analysed by FACSCalibur (BD Biosciences) and FCAP array software (BD Biosciences).

Intracellular cytokine staining and flow cytometric analysis. Purified CD4$^+$ T cells were stimulated with 10 μg/ml anti-CD3 and 10 μg/ml anti-CD28 for 48 h. Cells were collected and stimulated again with 50 ng/ml PMA and 750 nM ionomycin for 4 h in the presence of 10 μg/ml BFA. Cells were fixed and permeabilized by Cytofix/Cytoperm Fixation/Permeabilization solution (BD Biosciences; No. 554722) according to the manufacturer's instructions and then stained with APC-anti-IL-2. BMDC were stimulated with or without 1 μg/ml LPS for 24 h and stained with FITC-anti-CD80, PE-anti-CD86 and APC-anti-CD11c. Cells were analysed by FACSCalibur and Cell Quest software (BD Biosciences).

Quantitative real-time PCR. RNAs form total spleen cells, CD4$^+$ T cells and CD11c$^+$ DCs of hNFKBIL1-Tg and littermate control mice were prepared using TRIzol reagent (Invitrogen). Complementary DNA was synthesized by SuperscriptIII reverse transcriptase (Invitrogen) with random hexamer primer. Quantitative real-time PCR was performed using Fast SYBR Green Master Mix on an ABI Fast 7500 machine (Applied Biosystems, Carlsbad, CA, USA). Primers for hNFKBIL1 forward, 5′-TGGAGACAGAAGCTCCAGGGTGA-3′ and reverse, 5′- CGGGATCCCTCTGCTTCTCGC-3′ and mouse β-actin forward, 5′- GACGGCCAGGTCATCACTATTG-3′ and reverse, 5′- AGGAAGGCTGGAAAAGAGCC-3′ were used to evaluate the relative gene expression. The data were analysed by $\Delta\Delta$C method.

Statistical analyses. Difference between wild-type (WT) and Tg mice in CIA and CAIA experiments were analysed by Mann–Whitney *U*-test. Cell proliferation and cytokine production were compared with Student's *t*-test. All data are represented as mean ± SEM or SD where indicated. Values of $P < 0.05$ were considered statistically significant.

Results

NFKBIL1 suppressed the development of collagen-induced arthritis

To evaluate the role of NFKBIL1, we generated transgenic mouse lines expressing human NFKBIL gene under the control of CMV promoter. We detected transgene-derived transcripts in total spleen cells, CD4$^+$ T cells and CD11c$^+$ DCs of transgenic (Tg) mouse, but not of WT mouse (Fig. 1A). Endogenous NFKBIL1 was expressed in all tissues examined (data not shown). We noticed that

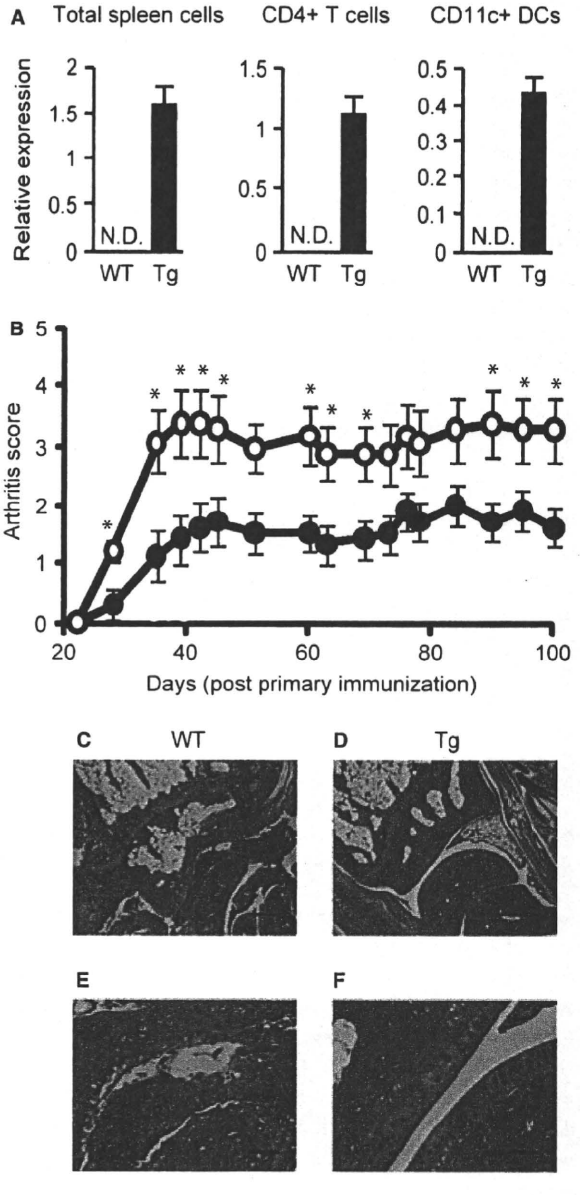

Figure 1 Reduced susceptibility of collagen-induced arthritis in NFKBIL1-Tg mice. (A) Expression of NFKBIL1 transgene in total spleen cells, CD4$^+$ T cells and CD11c$^+$ dendritic cells of NFKBIL1-Tg (n = 3) and WT littermates (n = 3) was analysed by quantitative RT-PCR. N.D., not detected. (B) NFKBIL1-Tg mice (closed circles) (n = 26) and WT littermates (open circles) (n = 83) with DBA/1j background were administered chicken type II collagen emulsified with CFA intradermally at the base of the tail on day 0. Three weeks later, mice were immunized again with CII/IFA. Severity of arthritis is shown. Similar results were obtained in two independent experiments, and one of them is demonstrated. (C–F) Joints of front limb of NFKBIL1-Tg (right) and WT littermate (left) mice at day 60 after primary immunization. Sections were stained with H&E. Scale bars represent 200 μm in (C, D) and 50 μm in (E, F). *$P < 0.05$.

transgene-carrying offspring were born at a smaller ratio than the expected Mendelian ratio in both of the two distinct Tg lines, suggesting some disadvantageous effect of the transgene on embryonic development. However, Tg mice grew normally after birth. Then, Tg mice had been backcrossed with a CIA-susceptible strain, DBA/1j, for more than seven generations. We examined the effect of enforced NFKBIL1 expression on the development of CIA, which is widely used as an experimental model for human RA. NFKBIL1-Tg mice and WT littermates immunized with type II collagen (C-II) with CFA were evaluated for arthritis severity. As shown in Fig. 1B, the severity of CIA was suppressed in NFKBIL1-Tg mice compared with WT control, although the kinetics of CIA development did not differ significantly. For example, swelling of front limbs was often observed in WT controls, but was rarely shown in NFKBIL1-Tg mice. A histological analysis of the front limb joints of WT controls showed typical features of arthritis, which were characterized by marked synovial and periarticular inflammation with cellular infiltration, synovial hyperplasia and pannus formation (Fig. 1C,E). In contrast, NFKBIL1-Tg mice showed no signs of synovial inflammation and cellular infiltration (Fig. 1D,F). Thus, the results indicated that NFKBIL1 was involved in the control of CIA pathogenesis.

Collagen antibody-induced arthritis was less, but still significantly suppressed by NFKBIL1

C-II-specific antibody production is considered to be crucial for CIA pathogenesis because antibody levels against C-II correlate well with the development of CIA [11]. Although NFKBIL1-Tg mice showed milder arthritis in CIA, C-II-specific IgG levels in sera did not differ from those in littermate control (Fig. 2). Thus, C-II-specific antibody production was not influenced by NFKBIL1. To examine whether antibody-mediated effector function was affected by NFKBIL1, CAIA was induced by the administration of a collagen-specific monoclonal antibody

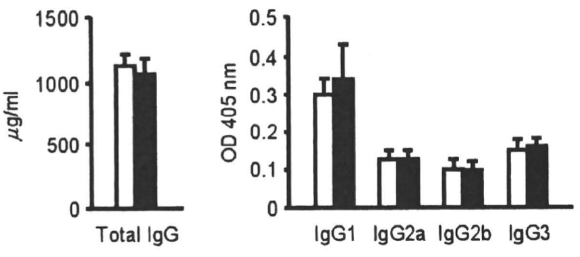

Figure 2 Comparable production of anti-CII antibodies. Sera of WT (open bars) and NFKBIL1-Tg (closed bars) mice were collected at day 30 after primary immunization of the collagen-induced arthritis procedure. The levels of serum antibodies against CII in each animal were measured by ELISA. Results are shown as averages ± SEM of 19 (WT) and 15 (Tg) mice.

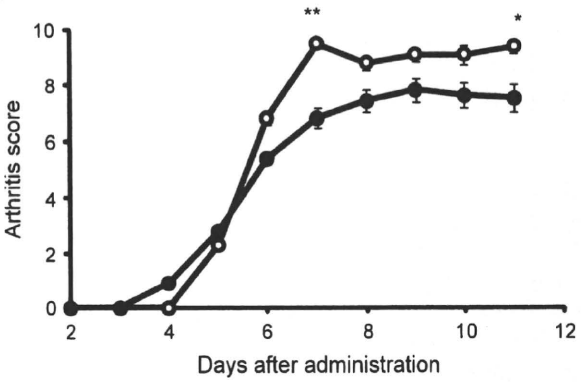

Figure 3 Less, but significant suppression of collagen antibody-induced arthritis in NFKBIL1-Tg mice. NFKBIL1-Tg (closed circles) (n = 9) and WT littermate (open circles) (n = 10) mice with DBA/1j background were i.p. administered a mixture of CII-specific antibodies. After 3 days, mice were i.p. administered LPS. Severity of arthritis score is shown. Data are shown as averages ± SEM. *P < 0.05, and **P < 0.01.

cocktail. In this experimental arthritis model, the induction phase of autoimmune reaction was bypassed. As shown in Fig. 3, arthritis severity was significantly reduced in NFKBIL1-Tg mice compared to WT controls, suggesting that the effector phase mediated by the administered antibody was impaired. However, the reduction in the severity was milder than that seen in CIA. Therefore, it was assumed that the induction phase was also affected by NFKBIL1.

Induction of immune responses was suppressed by NFKBIL1

To examine the role of NFKBIL1 in the early phase of immune responses, total spleen cells of non-immunized mice were stimulated with several mitogens such as ConA, LPS or anti-CD3 mAb and [^{3}H]-thymidine incorporation was measured (Fig. 4). Consistent with the above assumption that NFKBIL1 is involved in the induction phase of arthritis, spleen cells of naïve NFKBIL1-Tg mice showed decreased proliferation responding to mitogens.

Next, we evaluated the T cell functions of NFKBIL1-Tg mice. $CD4^+$ and $CD8^+$ T cells isolated from spleen were stimulated with anti-CD3 and CD28 antibodies and [^{3}H]-thymidine incorporation was measured. In contrast to the result of total spleen cells (Fig. 4), both $CD4^+$ and $CD8^+$ T cells of Tg mice showed greatly increased proliferation (Fig. 5A). Especially, $CD4^+$ T cell proliferation was four times higher in Tg mice than that in WT mice.

According to the expression profile of CD44 and CD25, $CD4^+$ T cells can be divided into $CD25^+$, $CD25^-CD44^{lo}$ and $CD25^-CD44^{hi}$ cells. Among them, $CD25^-CD44^{lo}$ cells can be regarded as naïve T cells and CD25-CD44hi cells as memory-phenotype T cells. It is known that naïve T cells and memory-phenotype T cells possess distinct functional properties [12]. In some

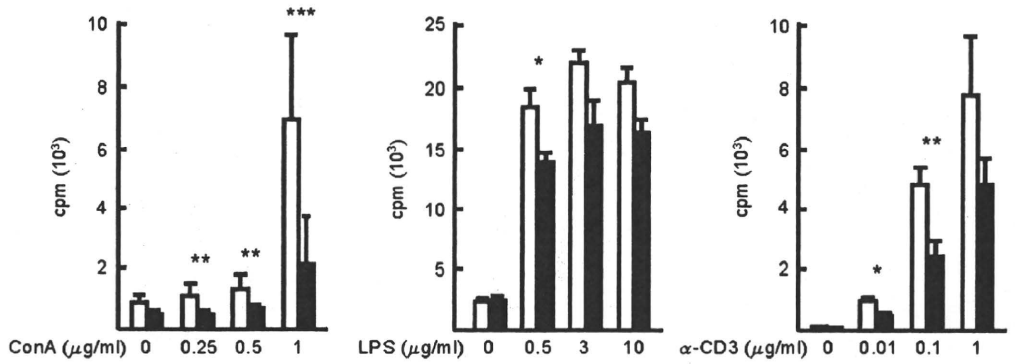

Figure 4 Decreased proliferative responses of spleen cells in NFKBIL1-Tg mice. Spleen cells (5×10^4 cells) of NFKBIL1-Tg (closed bars) and WT littermate (open bars) mice were stimulated with indicated concentrations of ConA (left), LPS (middle) or anti-CD3 antibody (right) for 48 h in 96-well round-bottom microtiter plates. Proliferative responses were estimated by incorporation of [^{3}H]-dT for the last 18 h and average value of three wells was calculated. Data are shown as averages ± SEM of 21 (WT) or 6 (Tg) mice. $*P < 0.05$, $**P < 0.01$ and $***P < 0.001$.

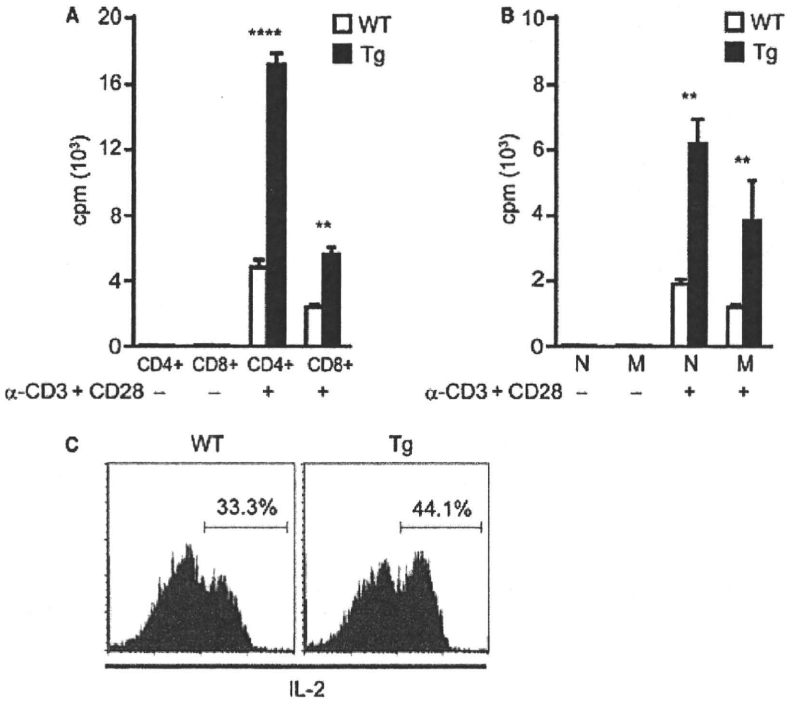

Figure 5 Increased proliferation and cytokine production of T cells in NFKBIL1-Tg mice. CD4$^+$ and CD8$^+$ T cells (A) and naïve ('N' in B) and memory-phenotype ('M' in B) CD4$^+$ T cells (1×10^4 cells) were cultured with or without plate-bound anti-CD3 antibody (5 μg/ml) and soluble anti-CD28 antibody (10 μg/ml) for 48 h. Proliferative responses were estimated by incorporation of [^{3}H]-dT for the last 18 h. Data are shown as averages ± SEM. $**P < 0.01$, $****P < 0.00001$. (C) Cytokine production was determined by staining for intracellular IL-2. CD4$^+$ T cells were stimulated with anti-CD3 (5 μg/ml) and CD28 (10 μg/ml) antibodies for 48 h in the presence of 10 μg/ml brefeldin A for the last 4 h. Following fixation, cells were stained with APC-conjugated anti-IL-2 antibody and analysed by FACSCalibur. Data are representative of three (A, B) or two (C) independent experiments.

studies, it was demonstrated that memory-phenotype T cells play pivotal roles in the induction of autoimmunity. Then, CD44^{lo} naïve and CD44^{hi} memory-phenotype T cells were separated and analysed.

In both naïve and memory-phenotype CD4$^+$ T cells, NFKBIL1-Tg T cells showed greater incorporation of [^{3}H]-thymidine than WT T cells (Fig. 5B). Consistent with this, IL-2 production was augmented in NFKBIL1-Tg T cells (Fig. 5C). These results clearly indicated that the reduced severity of arthritis in NFKBIL1-Tg mice did not result from impaired T cell functions.

APC functions for producing pro-inflammatory cytokines and activating T cells were impaired

The apparent discrepancy between the reduced proliferation of total spleen cells and enhanced T cell functions may be explained by the impairment of some other cell populations. Spleen cells depleted of both T and B cells were isolated from Tg mice and control mice. These non-T non-B cells were cultured with CD4$^+$ T cells either of Tg or control mice in the presence of anti-CD3 antibody and [^{3}H]-thymidine incorporation was measured. Either

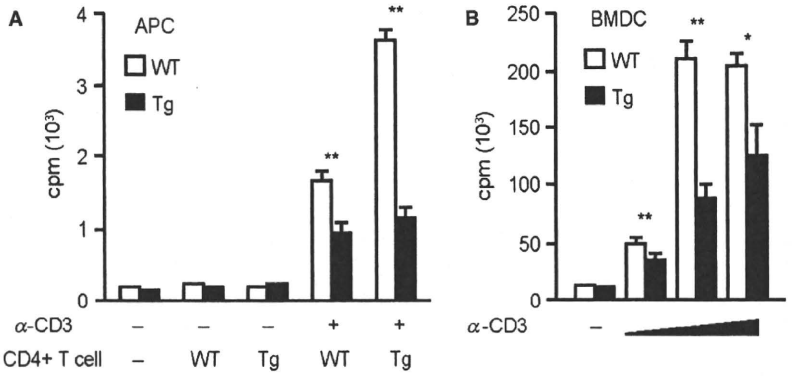

Figure 6 Impaired functions of APC in NFKBIL1-Tg mice. $CD4^+$ T cells (1×10^5 cells) were cultured with 1×10^4 cells of WT (open bars) or NFKBIL1-Tg (closed bars) splenic non-T non-B cells (A) or bone marrow-derived dendritic cells (BMDC) (B) in the presence or absence of anti-CD3 antibody at the indicated concentrations (0.01–10 μg/ml) for 48 h. Proliferative responses were estimated by incorporation of $[^3H]$-dT for last 18 h. Data are shown as averages ± SEM and representative of three independent experiments. $^*P < 0.05$, $^{**}P < 0.01$.

with Tg mouse T cells or with control mouse T cells, non-T non-B cells of Tg mice induced less prominent proliferation compared to those of control mice (Fig. 6A).

Because non-T non-B cell fraction contains large numbers of DC, the function of DC in Tg mice could be impaired. Indeed, bone marrow-derived DCs of Tg mice induced T cell proliferation less effectively than WT controls (Fig. 6B). In agreement with this, IL-2 production of T cells was decreased when T cells were cultured with DCs of Tg mice (data not shown). These observations suggested that the functions of APC, especially DCs, were impaired in NFKBIL1-Tg mice.

For optimal activation of T cells, the binding of CD28 on T cells with the B7 family on APC is required. Thus, we examined the expression levels of B7 family members, CD80 and CD86, on DCs after stimulation with LPS. CD80 and CD86 expressions were less prominently induced in Tg mouse BMDCs (Fig. 7A), while MHC class II expression was similar (data not shown). Next, we assessed the production of inflammatory cytokines. BMDC were stimulated with LPS for 24 h and the amounts of secreted cytokines were measured. NFKBIL1-Tg mouse BMDC produced less amounts of IL-6 and TNFα compared to WT control mice, while the

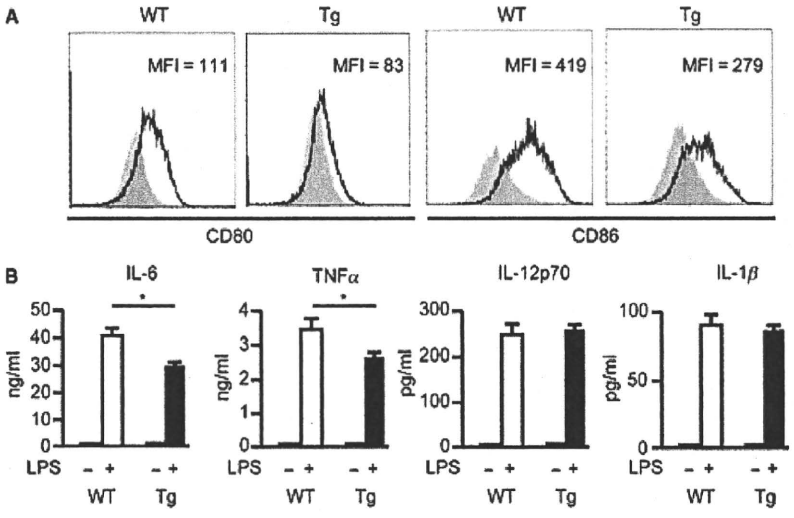

Figure 7 Reduced expression of effector molecules to elicit immune responses in NFKBIL1-Tg bone marrow-derived dendritic cells (BMDC). (A) BMDC (1×10^5 cells) were stimulated with (open histograms) or without (closed histograms) 1 μg/ml LPS for 24 h. Cells were stained with monoclonal antibodies specific for CD11c, CD80 and CD86 and then analysed by FACSCalibur. The magnitude of CD80 and CD86 expression in CD11c-positive cells was defined by mean fluorescence intensity (MFI). (B) WT (open bars) or hNFKBIL1-Tg (closed bars) BMDC (1×10^5 cells) were stimulated with or without 100 ng/ml LPS for 24 h. Secreted cytokine amounts were measured by CBA. The results are shown as averages ± SD. Data are representative of two independent experiments. $^*P < 0.05$.

productions of IL-1β and IL-12p70 were not significantly different (Fig. 7B). These results suggested that NFKBIL1 negatively regulated immune responses through, at least in part, the suppression of DC functions.

Discussion

In this study, we demonstrated that NFKBIL1 was involved in the control of experimental arthritis. This is the first report to validate the link between genetic evidence and the function of NFKBIL1 in the pathogenesis of arthritis. A to T substitution at position −62 in the promoter region of the NFKBIL1 gene locus was associated with the susceptibility to RA [7]. Shibata *et al.* [13] suggested that in addition to −62 T/A, other SNPs such as −422(T)8/(T)9, −325C/G and −263A/G were associated with susceptibility to RA pathogenesis and that patients harbouring this haplotype showed decreased expression of NFKBIL1. This seemed to be consistent with our present results that the forced expression of NFKBIL1 confers significant resistance to CIA and CAIA. Given that SNPs within the NFKBIL1 region are also associated with chronic thromboembolic pulmonary hypertension, Takayasu's arteritis and type I diabetes among Japanese, and ulcerative colitis, SLE and Sjogren's syndrome in Caucasians, NFKBIL1 may be broadly involved in autoimmune disorders [13–17]. More than 92% of NFKBIL1 amino acid sequence is identical between human and mouse. Especially, ankyrin repeat region is 100% identical. This suggests that NFKBIL1 plays some important roles beyond species. Indeed, NFKBIL1-deficient mice showed earlier onset of CIA (our unpublished observation), consistent with the finding in this study that over-expression of human NFKBIL1 reduced severity of experimental autoimmune arthritis.

T cells play pivotal roles in various aspects of autoimmunity. However, isolated $CD4^+$ and $CD8^+$ T cells of hNFKBIL1-Tg mice showed enhanced responses to anti-CD3 plus anti-CD28 stimulation. This seemed inconsistent with the reduced severity of CIA in Tg mice. Because it was reported that memory-like phenotype T cells often contributed to autoimmune aetiology [12], we examined the $CD4^+44^{hi}$ memory-phenotype T cells in hNFKBIL1-Tg mice. However, the response to mitogenic stimuli of both memory-phenotype and naïve $CD4^+$ T cells was enhanced in Tg mice. Therefore, the lesser susceptibility to induced arthritis in hNFKBIL1-Tg mice was not attributed to impaired T cell functions, indicating that some other cell types caused the reduction in arthritis severity.

In hNFKBIL1-Tg mice, CIA severity was significantly suppressed, although the production of antibodies against C-II was comparable to that in littermate control mice. Reduced severity of arthritis was also observed in CAIA. It was previously reported that RAG-deficient mice showed comparable severity of CAIA especially in the early phase [18], indicating that innate immune cells play important roles in the development of CAIA. Therefore, we assumed that the effector functions mediated by innate immune cells were suppressed in Tg mice. Because elicitation of T cell responses requires various innate APC, dysfunctions of APC in Tg mice would result in reduced T cell responses. In this study, we showed that APC in Tg mice supported T cell proliferation less efficiently than control mouse APC. Impaired functions of APC seemed to contribute to the decreased proliferation of total spleen cells in spite of enhanced proliferative capability of T cells in Tg mice.

We found that the expressions of co-stimulatory molecules, CD80/86, were inefficiently induced by LPS in BMDC of Tg mice and that LPS-induced inflammatory cytokine production, such as that of IL-6 and TNFα, was reduced in Tg mice. It was reported that the blockade of co-stimulatory molecule engagement by gene targeting or administration of neutralizing antibodies inhibited CIA progression [19, 20], and that TNFα was essential for CAIA [21]. Our observations seemed consistent with these previous reports.

NF-κB is one of the important downstream targets of Toll-like receptor (TLR)-mediated signalling, which is elicited by LPS. It is well known that inflammatory cytokine production and DC maturation including CD80/CD86 up-regulation requires NF-κB activation [22]. Because the ankyrin repeat region in NFKBIL1 protein exhibits significant homology with the region in IκB family proteins, such as IκBα, it is plausible that NFKBIL1 is involved in the modification of NF-κB signalling pathway in innate immune cells. However, unlike conventional IκBs that localize in the cytoplasm, NFKBIL1 resides in the nucleus [23]. In recent years, it was reported that several atypical IκB family members, such as IκBNS and Bcl-3, are localized in the nucleus and that selectively suppressed the transcription of IL-6 and TNFα, respectively [24, 25]. It is of note that NFKBIL1 affected the expressions of inflammatory cytokines in a context-dependent manner; the expressions of IL-6 and TNFα were repressed in Tg mouse BMDC, while those of IL-1β and IL-12 were not altered (Fig. 7B). It is assumed that NFKBIL1 modified NF-κB-mediated gene expression in a similar way to atypical IκB family members.

It was reported that one of the atypical IκB, IκBNS, suppressed the production of IL-6 and IL-12 in APCs but was required for IL-2 production in T cells [26, 27]. Similarly, we found that over-expression of NFKBIL1 reduced production of IL-6 and TNFα in BMDC and enhanced T cell responses including proliferation and IL-2 production. It was suggested these nuclear IκBs are differently involved in the control of target genes according to the cell types. On the other hand, Greetham *et al.*

[10] showed that NFKBIL1 did not modulate NF-κB signalling in an NF-κB reporter assay and also demonstrated that NFKBIL1 bound to some RNA processing factors, raising the possibility that NFKBIL1 is involved in post-transcriptional regulation. The reason for the discrepancy is not clear. Further studies are needed to clarify the molecular mechanisms of how NFKBIL1 affects the pathogenesis of various autoimmune diseases.

In conclusion, NFKBIL1 is involved in RA pathogenesis, partly through the control of DC functions including inflammatory cytokine production and supporting T-cell responses.

Acknowledgment

This work was supported by 2008 Tokai University School of Medicine Project Research to T. Sato.

References

1 Firestein GS. Evolving concepts of rheumatoid arthritis. *Nature* 2003;423:356–61.
2 Leung BP, Conacher M, Hunter D, McInnes IB, Liew FY, Brewer JM. A novel dendritic cell-induced model of erosive inflammatory arthritis: distinct roles for dendritic cells in T cell activation and induction of local inflammation. *J Immunol* 2002;169:7071–7.
3 McInnes IB, Schett G. Cytokines in the pathogenesis of rheumatoid arthritis. *Nat Rev Immunol* 2007;7:429–42.
4 Yap DY, Lai KN. Cytokines and their roles in the pathogenesis of systemic lupus erythematosus: from basics to recent advances. *J Biomed Biotechnol* 2010;2010:365083.
5 Renner F, Schmitz ML. Autoregulatory feedback loops terminating the NF-kappaB response. *Trends Biochem Sci* 2009;34:128–35.
6 van der Helm-van Mil AH, Wesoly JZ, Huizinga TW. Understanding the genetic contribution to rheumatoid arthritis. *Curr Opin Rheumatol* 2005;17:299–304.
7 Okamoto K, Makino S, Yoshikawa Y *et al.* Identification of I kappa BL as the second major histocompatibility complex-linked susceptibility locus for rheumatoid arthritis. *Am J Hum Genet* 2003;72:303–12.
8 Lin CH, Cho CL, Tsai WC *et al.* Inhibitors of kB-like gene polymorphisms in rheumatoid arthritis. *Immunol Lett* 2006;105:193–7.
9 Handel-Fernandez ME, Vincek V. Sequence analysis and expression of a mouse homolog of human IkappaBL gene. *Biochim Biophys Acta* 1999;1444:306–10.
10 Greetham D, Ellis CD, Mewar D *et al.* Functional characterization of NF-kappaB inhibitor-like protein 1 (NFkappaBIL1), a candidate susceptibility gene for rheumatoid arthritis. *Hum Mol Genet* 2007;16:3027–36.
11 Seki N, Sudo Y, Yoshioka T *et al.* Type II collagen-induced murine arthritis. I. Induction and perpetuation of arthritis require synergy between humoral and cell-mediated immunity. *J Immunol* 1988;140:1477–84.
12 King C, Ilic A, Koelsch K, Sarvetnick N. Homeostatic expansion of T cells during immune insufficiency generates autoimmunity. *Cell* 2004;117:265–77.
13 Shibata H, Yasunami M, Obuchi N *et al.* Direct determination of single nucleotide polymorphism haplotype of NFKBIL1 promoter polymorphism by DNA conformation analysis and its application to association study of chronic inflammatory diseases. *Hum Immunol* 2006;67:363–73.
14 Yamashita T, Hamaguchi K, Kusuda Y, Kimura A, Sakata T, Yoshimatsu H. IKBL promoter polymorphism is strongly associated with resistance to type 1 diabetes in Japanese. *Tissue Antigens* 2004;63:223–30.
15 de la Concha EG, Fernandez-Arquero M, Lopez-Nava G *et al.* Susceptibility to severe ulcerative colitis is associated with polymorphism in the central MHC gene IKBL. *Gastroenterology* 2000;119:1491–5.
16 Castiblanco J, Anaya JM. The IkappaBL gene polymorphism influences risk of acquiring systemic lupus erythematosus and Sjogren's syndrome. *Hum Immunol* 2008;69:45–51.
17 Kominami S, Tanabe N, Ota M *et al.* HLA-DPB1 and NFKBIL1 may confer the susceptibility to chronic thromboembolic pulmonary hypertension in the absence of deep vein thrombosis. *J Hum Genet* 2009;54:108–14.
18 Wang J, Fathman JW, Lugo-Villarino G *et al.* Transcription factor T-bet regulates inflammatory arthritis through its function in dendritic cells. *J Clin Invest* 2006;116:414–21.
19 Tada Y, Nagasawa K, Ho A *et al.* CD28-deficient mice are highly resistant to collagen-induced arthritis. *J Immunol* 1999;162:203–8.
20 Iwai H, Kozono Y, Hirose S *et al.* Amelioration of collagen-induced arthritis by blockade of inducible costimulator-B7 homologous protein costimulation. *J Immunol* 2002;169:4332–9.
21 Kagari T, Doi H, Shimozato T. The importance of IL-1 beta and TNF-alpha, and the noninvolvement of IL-6, in the development of monoclonal antibody-induced arthritis. *J Immunol* 2002;169:1459–66.
22 Kaisho T, Akira S. Dendritic-cell function in Toll-like receptor- and MyD88-knockout mice. *Trends Immunol* 2001;22:78–83.
23 Semple JI, Brown SE, Sanderson CM, Campbell RD. A distinct bipartite motif is required for the localization of inhibitory kappaB-like (IkappaBL) protein to nuclear speckles. *Biochem J* 2002;361:489–96.
24 Hirotani T, Lee PY, Kuwata H *et al.* The nuclear IkappaB protein IkappaBNS selectively inhibits lipopolysaccharide-induced IL-6 production in macrophages of the colonic lamina propria. *J Immunol* 2005;174:3650–7.
25 Kuwata H, Watanabe Y, Miyoshi H *et al.* IL-10-inducible Bcl-3 negatively regulates LPS-induced TNF-alpha production in macrophages. *Blood* 2003;102:4123–9.
26 Kuwata H, Matsumoto M, Atarashi K *et al.* IkappaBNS inhibits induction of a subset of Toll-like receptor-dependent genes and limits inflammation. *Immunity* 2006;24:41–51.
27 Touma M, Antonini V, Kumar M *et al.* Functional role for I kappa BNS in T cell cytokine regulation as revealed by targeted gene disruption. *J Immunol* 2007;179:1681–92.

Human Immunology 72 (2011) 269–272

Contents lists available at ScienceDirect

journal homepage: www.elsevier.com/locate/humimm

Association analysis of Toll-like receptor 7 gene polymorphisms and Behçet's disease in Japanese patients

Toshiro Sada [a], Masao Ota [b,*], Yoshihiko Katsuyama [c], Akira Meguro [a], Eiichi Nomura [a], Riyo Uemoto [a], Tadayuki Nishide [a], Eiichi Okada [d], Shigeaki Ohno [e], Hidetoshi Inoko [f], Nobuhisa Mizuki [a]

[a] Department of Ophthalmology and Visual Science, Yokohama City University, Graduate School of Medicine, Kanagawa, Japan
[b] Department of Legal Medicine, Shinshu University School of Medicine, Nagano, Japan
[c] Department of Pharmacy, Shinshu University Hospital, Nagano, Japan
[d] Okada Eye Clinic, Kanagawa, Japan
[e] Department of Ophthalmology and Visual Sciences, Hokkaido University, Graduate School of Medicine, Hokkaido, Japan
[f] Department of Molecular Life Science, Division of Molecular Medical Science and Molecular Medicine, Tokai University School of Medicine, Kanagawa, Japan

ARTICLE INFO

Article history:
Received 28 September 2010
Accepted 8 December 2010
Available online 14 December 2010

Keywords:
Behçet's disease
Association
TLR7 polymorphism

ABSTRACT

Action of Toll-like receptors (TLRs) is deeply associated with defense mechanisms of the innate and adaptive immune responses to microbial pathogens. There have been reports of genetic polymorphisms within the TLR7 gene being closely related to a variety of inflammatory and infectious diseases. Behçet's disease (BD) is an autoinflammatory disease, and the pathogenesis has yet to be fully discovered. We investigated whether polymorphisms of Toll-like receptor 7 (TLR7) are associated with BD by analyzing the frequency of eight single nucleotide polymorphisms (SNPs) within 200 Japanese BD patients and 102 randomized controls. We genotyped nine SNPs in the TLR7 gene and assessed the allele/genotype diversity between cases and controls for all SNPs. In all eight SNPs, statistically significant differences were not observed between cases and controls.

1. Introduction

Toll-like receptors (TLRs) are a class of evolutionarily conserved pathogen recognition receptors that play an important role in innate identification of foreign material. Activating TLR induces both the innate and adaptive immune reactions against invading pathogens [1–3]. Particularly, genetic variables in genes related to innate immunity are associated with a series of inflammatory disorders [4].

TLR7 is expressed in various human cells, most commonly in plasmacytoid dendritic cells (pDCs) and B cells. TLR7 identifies single strand RNA (ssRNA) and antiviral drugs, such as Imiquimod, the family of synthetic small nucleotid-like molecules of imadazoquinolinamines [5–9]. Th1 cytokines, such as interferon-α or interleukin-12, and Th1 biased immune response is induced by activation of TLR7 in pDC [10].

The TLR7 gene, found on chromosome Xp22.3, has three exons, two of which have coding function, and spans 155 [10].

Behçet's disease (BD) is a recurrent systemic inflammatory disorder characterized by four major pathognomonic symptoms: recurrent uveoretinitis, oral aphthosis, genital ulcers, and skin lesions, which may continue a few days to several weeks, some of them leaving temporary tissue damage and causing chronic symptoms or even death [11]. On occasion, BD is concomitant with tissue and organ inflammation throughout the body, including the vascular system, gastrointestinal tract, central nervous system, lungs, kidneys, joints, and epididymis [12]. This disease is most common in young adults, although there have been reports of childhood onset [13]. BD is considered more prevalent in Mongoloid but rarely in Caucasian populations, with a particularly high frequency in areas along the old silk trading routes from Japan to the Middle East and the Mediterranean basin [14]. However, BD is not restricted to persons in these regions.

Although it is still uncertain why the immune system starts to behave this way in BD, various genetic and environmental factors, Immune mechanisms, and infectious agents are thought to affect the onset of BD. The association between BD and human leukocyte antigen class I antigen, HLA-B51 has been proved with evidence. Furthermore, we suggest that HLA-B*51 allele is a possible candidate to indicate susceptibility of developing BD [15]. Streptococcal antigens [16], bacterial super-antigens [17], mycobacterial antigens [18], and type 1 herpes virus [19] were also discovered to be contributory factors to BD development. Varani et al. suggested that human cytomegalovirus (HCM) induces IFN-α secretion from plasmacytoid dendritic cells, which is the main inducers of the type 1 IFN in response to viral infection, through engagement of the TLR7 pathways [20]. Moreover, the implication of TLR7 was introduced in the recognition of DNA virus, such as herpesvirus in mice [21].

* Corresponding author.
E-mail address: otamasao@sch.md.shinshu-u.ac.jp (M. Ota).

0198-8859/11/$32.00 - see front matter © 2011 American Society for Histocompatibility and Immunogenetics. Published by Elsevier Inc. All rights reserved.
doi:10.1016/j.humimm.2010.12.007

Table 1
Association analysis of TLR7 SNPs

dbSNP	Name	Allele	Gender												
			Combined					Female					Male			
			case (n = 200)	control (n = 102)	O.R.	p	p^a	case (n = 84)	control (n = 54)	O.R.	p	p^a	case (n = 116)	control (n = 48)	O.R.	p
rs5935436	SNP1	C	199	101	1.97			84	53	4.74			115	48	–	
		T	6	8	0.37	0.058		5	8	0.38	0.082		1	0	–	
rs5741880	SNP2	G	199	101	1.97			84	53	4.74			115	48	–	
		T	6	8	0.37	0.058		5	8	0.38	0.082		1	0	–	
rs5743733	SNP3	C	190	101	0.19	0.078		82	53	0.93			108	48	–	0.062
		G	17	15	0.54	0.097		9	15	0.31	**0.010**		8	0	–	0.062
		C/C	183	87	1.86	0.097		75	39	3.21	**0.010**					
		C/G	7	14	0.23	**0.002**	**0.004**	7	14	0.26	**0.005**	**0.035**				
		G/G	10	1	5.32			2	1	1.29	0.697					
rs5743740	SNP4	A	182	94	0.86			84	52	–	0.076		98	42	0.78	
		G	41	21	0.99			23	15	0.98			18	6	1.29	
rs179016	SNP5	G	182	94	0.86			84	52	8.05	0.076		98	42	0.78	
		C	41	22	0.99			23	16	0.89			18	6	1.29	
rs1620233	SNP6	C	194	101	0.32			84	54	1.55			110	47	0.39	
		T	15	4	1.99			9	3	1.85			6	1	2.56	
rs179012	SNP7	G	187	94	1.22			84	53	4.74			103	41	1.35	
		A	29	21	0.65			16	14	0.67			13	7	0.74	
rs3853839	SNP8	G	67	43	0.69			39	22	1.25			28	21	0.41	**0.013**
		A	169	76	1.87	**0.036**		81	49	2.59			88	27	2.44	**0.013**

Only p values < 0.1 are included in the table. p values < 0.05 are indicated in bold type. p and p^a values were calculated by χ^2 test 2 × 2 and 3 × 2 contingency table, respectively. SNP: reference SNP number from the dbSNP database. O.R.: odds ratio.

The role of TLR7 in the pathogenesis of Behçet's disease remains uncertain, but the herpes simplex virus DNA was actually detected in saliva of patients with BD [22].

There have been numerous reports on investigations of the association between TLR7 polymorphisms and diseases such asthma [23], age-related macula degeneration [24], and systemic lupus erythematosus [25,26]. However, a genetic study on the relationship of TLR7 polymorphisms and BD has yet to be reported. The present study was undertaken to investigate the relationship between TLR7 single nucleotide polymorphisms (SNPs) and BD, and to evaluate the potential candidacy of TLR7 as a BD susceptibility gene by case-control analysis.

2. Subjects and methods

The total subject group consisted of 200 Japanese patients diagnosed with BD and 102 healthy Japanese control subjects. The BD patients were diagnosed according to the standard criteria proposed by the Japan Behçet's Disease Research Committee at the Uveitis Clinic of Yokohama City University or Hokkaido University and classified as complete-type BD or incomplete-type BD, according to these criteria [27]. All the control subjects were healthy volunteers and similar in ethnic origin to the patients; control subjects were unrelated to each other and to the BD patients. The research methods were in compliance with the Declaration of Helsinki guidelines. Details of the study were explained to all patients and controls, and consent to genetic screening was obtained. Peripheral blood lymphocytes were collected, and genomic DNA was extracted from peripheral blood cells using the QIAamp DNA Blood Maxi Kit (Qiagen, Valencia, CA.)

2.1. TLR7 genotyping

Eight SNPs (rs5935436, rs5741880, rs5743733, rs5743740, rs179016, rs1620233, rs179012, and rs3853839; named SNP1-SNP8) within the TLR7 gene were genotyped by the TaqMan 5′ exonuclease assay using primers supplied by Applied Biosystems (Foster City, CA). Probe fluorescence signal was detected by TaqMan, Assay for Real-Time PCR (7500 Real Time PCR System; Applied Biosystems) following the manufacturer's instructions.

2.2. Statistical analysis

Allelic frequencies of all detected SNPs were tested for Hardy–Weinberg equilibrium. Differences of genotype frequency between case and control were assessed by Chi-squared test and Fisher's exact test. The maximum likelihood estimates of haplotype frequencies were estimated by pairs of unphased genotypes using the expectation–maximization algorithms in the R package "haplo.stats" [28]. Statistical analyses were performed by the STATVIEW software (version 5.0; SAS Institute, Inc., Cary, NC). The correction of p values (p_c) was calculated by the Bonferroni's correction when the coefficient was the total number of the contingency tables tested. A p value <0.05 and p_c value <0.01 were considered as statistically significant. The strength of linkage disequilibrium (LD)

Table 2
Pairwise Linkage Disequilibrium Between SNPs in Cases and Controls Groups

		SNP1 rs5935436	SNP2 rs5741880	SNP3 rs5743733	SNP4 rs5743740	SNP5 rs179016	SNP6 rs1620233	SNP7 rs179012	SNP8 rs3853839
SNP1	rs5935436		1 (1)	1 (0.54)	0.06 (0.001)	0.04 (0.001)	1 (0.002)	0.08 (0.002)	1 (0.03)
SNP2	rs5741880	1 (1)		1 (0.54)	0.06 (0.001)	0.04 (0.001)	1 (0.002)	0.08 (0.002)	1 (0.03)
SNP3	rs5743733	1 (0.3)	1 (0.3)		1 (0.02)	1 (0.02)	1 (0.003)	0.99 (0.02)	1 (0.05)
SNP4	rs5743740	0.07 (0.001)	0.07 (0.001)	1 (0.01)		1 (0.95)	0.67 (0.07)	0.78 (0.58)	0.1 (0.001)
SNP5	rs179016	0.07 (0.001)	0.07 (0.001)	1 (0.01)	1 (1)		1 (0.15)	0.78 (0.58)	0.15 (0.002)
SNP6	rs1620233	1 (0.001)	1 (0.001)	1 (0.004)	1 (0.33)	1 (0.33)		0.28 (0.00)	1 (0.01)
SNP7	rs179012	0.43 (0.00)	0.43 (0.00)	1 (0.008)	0.75 (0.38)	0.75 (0.38)	1 (0.006)		0.15 (0.002)
SNP8	rs3853839	1 (0.007)	1 (0.007)	1 (0.02)	0.13 (0.006)	0.13 (0.009)	0.24 (0.001)	0.18 (0.01)	

The value in parenthesis shows Pearson correction (r^2).
The values in the upper right triangle and the lower left triangle are controls and cases respectively.

Table 3
Estimated haplotype frequencies of the TLR7 gene

Haplotype	SNP1-SNP8	Frequency, %				p (Female)	p (Male)
		Female		Male			
		Case n = 84	Control n = 54	Case n = 116	Control n = 48		
HP1	CGCAGCGG	55.01	48.65	58.62	43.75	0.301	0.082
HP2	CGCAGCGC	38.75	19.71	17.24	39.58	0.509	0.002
HP3	CGCGCCAG	5.41	7.67	3.44	6.25	0.451	0.419
HP4	CGCGCTGG	3.88	0.94	4.31	2.08	0.144	0.490
HP5	CGGAGCGG	3.57	6.48	6.03	0	0.265	0.082
HP6	CGCAGCAG	2.63	0.95	1.72	4.17	0.327	0.356
HP7	TTGAGCGG	2.02	6.60	0.86	0	0.053	0.519
HP8	CGCGCCAC	0.7	1.67	6.03	4.17	0.447	0.633

p values were calculated with the c2 test using a 2 × 2 contingency table.
p (Female) represents cases versus controls in female group.
p (male) represents cases versus controls in male group.

between SNPs was measured with LD coefficient (Lewontin's D′) [29], obtained from the R package "genetics" in the R Project for Statistical Computing (http://www.r-project.org/).

3. Results

Seven SNPs in TLR7 genotypes (SNP1, SNP2, SNP3, SNP4, SNP5, SNP6, and SNP7) were in the intron, and SNP8 in the UTR3 region. Allele frequencies of eight SNPs in cases and controls are shown in (Table 1). The allele frequencies of the eight SNPs in BD patients and controls showed no significant differences.

Because TLR7 is located on the X chromosome, we analyzed females and males separately as well as combined (female and male). In the female group, BD patients had a lower frequency of minor allele G ($p = 0.0099$), a higher frequency of genotype C/C ($p = 0.0099$) and C/G ($p = 0.005$), whereas frequency of major allele C and genotype G/G were not significantly different compared with those of the control. However, these differences in minor allele G, genotypes C/C and C/G were evaluated insignificant by Bonferroni's correction (Table 1). These associations were found for SNPs in the combined group. In the male group, a difference was observed in SNP8 (rs3853839) allele frequency ($p = 0.0125$). However this also was evaluated to be insignificant by Bonferroni's correction (Table 1).

The Hardy–Weinberg exact test was performed on the subjects used in this study, showing no genetic bias for each SNP.

The LD indexes in both controls and patients were also examined for the characteristic LD block using eight SNPs in TLR7 (Table 2). The pattern of LD block was similar between the case and the control group. The haplotype frequencies in BD patients and controls showed no suggestive difference (Table 3).

4. Discussion

Although the full etiology of BD is yet to be discovered, herpes simplex virus immunopathology, autoimmunity to oral mucosa, or cross-reactive microbial antigens and streptococcal infection are thought to be candidates in triggering BD. In addition, there is a possibility that antigens, such as ss-RNA virus and self DNA influence TLR7 mechanism, and in consequence, affect the development and severity of BD. TLR7 has an essential function in induction of intracellular defense mechanism of the innate immune system and activates effective adaptive immune responses against viral pathogens. Recently, the involvement of TLR7 in the sensing of and defense against infection with a herpes DNA virus was demonstrated [21] in mice. Moreover, the polymorphisms in the TLR7 gene was speculated as an influence to the functional capability of TLR7 to induce sufficient defense mechanism against microbial agents, rendering a high susceptibility to microbial attacks [30–32]. Results of the study were not able to support clearly the hypothesis of TLR7 gene being a susceptibility marker for BD, although allele frequency differences in different SNPs (in SNP 8:rs3853839 in men, and in SNP 3:rs5743733 in women) were shown. This equivocal evidence will be proved by further association studies using more samples and other groups.

This study in a group of Japanese subjects concludes that there is no suggestive relationship between TLR7 gene polymorphisms and susceptibility to BD. This theme is subject to further investigation with additional subjects in other ethnic populations.

References

[1] Akira S, Takeda K, Kaisho T. Toll-like receptors: Critical proteins linking innate and acquired immunity. Nat Immunol 2001;2:675–80.
[2] Andreakos E, Foxwell B, Feldmann M. Is targeting Toll-like receptors and their signaling pathway a useful therapeutic approach to modulating cytokine-driven inflammation? Immunol Rev 2004;202:250–65.
[3] Kang SS, Kauls LS, Gaspari AA. Toll-like receptors: Applications to dermatologic disease. J Am Acad Dermatol 2006;54:951–83.
[4] Lazarus R, Vercelli D, Palmer LJ, Klimecki WJ, Silverman EK, Richter B, et al. Single nucleotide polymorphisms in innate immunity genes: Abundant variation and potential role in complex human disease. Immunol Rev 2002; 190:9–25.
[5] Akira S, Takeda K. Toll-like receptor signaling. Nat Rev Immunol 2004;4:499–511.
[6] Takeda K, Kashio T, Akira S. Toll-like receptors. Annu Rev Immunol 2003;21: 335–76.
[7] Jurk M, Heil F, Vollmer J, Schetter C, Krieg AM, Wagner H, et al. Human TLR7 or TLR8 independently confer responsiveness to the antiviral compound R–848. Nat Immunol 2002;3:499.
[8] Hemmi H, Kaisho T, Takeuchi O, Sato S, Sanjo H, Hoshino K, et al. Small anti-viral compounds activate immune cells via the TLR7 MyD88-dependent signaling pathway. Nat Immunol 2002;3:196–200.
[9] Asslin-Paturel C, Trinchieri G. Production of type 1 interferons: Plasmacytoid dendritic cells and beyond. J Exp Med 2005;202:461–5.
[10] Du X, Poltorak A, Wei Y, Beutler B. Three novel mammalian Toll-like receptors: Gene structure, expression, and evolution. Eur Cytokine Netw 2000;11:362–71.
[11] Gul A. Behcet's disease as an autoinflammatory disorder. Curr Drug Targets Inflamm Allergy 2005;4:81–3.
[12] Kaklamani VG, Vaiopoulos G, Kaklamanis PG. Behxcet's disease. Semin Arthritis Rheum 1998;27:197–217.
[13] Bang D, Lee JH, Lee ES, Lee S, Choi JS, Kim YK, et al. Epidemiologic and clinical survey of Behcet's disease in Korea: The first multicenter study. J Korean Med Sci 2001;16:615–8.
[14] Ohno S, Ohguchi M, Hirose S, Matsuda H, Wakisaka A, Aizawa M. Close association of HLA-Bw51 with Behcet's disease. Arch Ophthalmol 1982;100:1455–8.
[15] Mizuki N, Ota M, Katsuyama Y, Yabuki K, Ando H, Shiina T, et al. HLA-B*51 allele analysis by the PCR-SBT method and a strong association of HLA-B*5101 with Japanese patients with Behcet's disease. Tissue Antigens 2001;58:181–4.
[16] Lehner T, Lavery E, Smith R, van der Zee R, Mizushima Y, Shinnick T. Association between the 65-kilodalton heat shock protein, Streptococcus sanguis, and the corresponding antibodies in Behcet's syndrome and the corresponding antibodies in Behcet's syndrome. Infect Immun 1991;59:1434–41.
[17] Hirohata S, Hashimoto T. Abnormal T cell responses to bacterial superantigens in Behcet's disease (BD). Clin Exp Immunol 1998;112:317–24.
[18] Direskeneli H, Eksioglu-Demiralp E, Yavuz S, Ergun T, Shinnick T, Lehner T, et al. T cell responses to 60/65 kDA heat shock protein derived peptides in Turkish patients with Behcet's disease. J Rheumatol 2000;27:708–13.
[19] Young C, Lehner T, Barnes CG. CD4 and CD8 cell responses to herpes simplex virus in Behcet's disease. Clin Exp Immunol 1998;73:6–10.
[20] Varani S, Cederav M, Feld S, Tammik C, Frascaroli G, Landini MP, et al. Human cytomegalovirus differentially controls B cell and T cell responses through effects on plasmacytoid dendritic cells. J Immunol 2007;179:7767–76.

[21] Zucchini N, Bessou G, Traub S, Robbins SH, Uematsu S, Akira S, et al. Cutting Edge: Overlapping functions of TLR7 and TLR9 for innate defense against a herpesvirus infection. J Immunol 2008;180:5799–803.
[22] Lee S, Bang D, Cho YH, Lee ES, Sohn S. Polymerase chain reaction reveals herpes simplex virus DNA in saliva of patients with Behcet's disease. Arch Dermatol Res 1996;288:179–83.
[23] Møller-Larsen S, Nyegaard M, Haagerup A, Vestbo J, Kruse TA, Børglum AD. Association analysis identifies TLR7 and TLR8 as novel risk genes in asthma and related disorders. Thorax 2008;63:1064–9.
[24] Edwards AO, Chen D, Fridley BL, James KM, Wu Y, Abecasis G, et al. Toll-like receptor polymorphisms and age-related macular degeneration. Invest Ophthalmol Vis Sci 2008;49:1652–9.
[25] Ptacek T, Li X, Kelley JM, Edberg JC. Copy number variants in genetic susceptibility and severity of systemic lupus erythematosus. Cytogenet Genome Res 2008;123:142–7.
[26] García-Ortiz H, Velázquez-Cruz R, Espinosa-Rosales F, Jiménez-Morales S, Baca V, Orozco L. Association of TLR7 copy number variation with susceptibility to childhood-onset systemic lupus erythematosus in Mexican population. Ann Rheum Dis 2010;69:1861–5.
[27] International Study Group for Behcet's disease. Criteria for the diagnosis of Behcet's disease. Lancet 1990; 335:1078–80.
[28] Schaid DJ, Rowland CM, Tines DE, Jacobson RM, Poland GA. Score tests for association between traits and haplotypes when linkage phase is ambiguous. Am J Hum Genet 2002;70:425–34.
[29] Lewontin RC. The interaction of selection and linkage. I. General considerations; heterotic models. Genetics 1964;49:49–67.
[30] Triantafilou K, Vakakis E, Orthopoulos G, Ahmed MA, Schumann C, Lepper PM, Triantafilou M. TLR8 and TLR7 are involved in the host's immune response to human parechovirus. Eur J Immunol 2005;35:2416–23.
[31] Koyama S, Ishii KJ, Kumar H, Tanimoto T, Coban C, Uematsu S, et al. Differential role of TLR- and RLR-signaling in the immune responses to influenza A virus infection and vaccination. J Immunol 2007;179:4711–20.
[32] Lenert PS. Classification, mechanisms of action, and therapeutic applications of inhibitory oligonucleotides for Toll-like receptors (TLR) 7 and 9. Mediat Inflamm 2010;2010:986596.